Dynamics of Compound Droplets: Rolling and Evaporation

by
Muhammad Rizwanur Rahman

A thesis submitted in partial fulfillment of the requirements for the degree of

Master of Science

Department of Mechanical Engineering
University of Alberta

Abstract

Superior control of multiphase micro-drops owns much of the future in microfluidic technology. Understanding the dynamics of such compound systems is the key to its large-scale applications. Interfacial interaction of a droplet at a liquid-fluid interface dictates its successful generation and stability. The knowledge of the interface dynamics creates a rich profusion of domains that were previously unexplored. The century-old power law, which was believed to be universal in governing temporal drop spreading on solid substrates, is seen to fail in predicting spreading on liquid-fluid interface. Rather a coalescence like behavior becomes imminent. The study of the fundamental physics of evaporation of double emulsion droplets and under liquid rolling dynamics are extensions of the successful generation technique. In contrast to the rigid body motion, dissipation inside and outside of a deformable drop always results in convoluted physics. While rolling on an incline, single-phase drops travel slower with increase in size. But a concealed direct dependency between the drop size and traveling velocity can be exposed by merely altering the medium resistance. Rolling motion of double emulsion droplets even affirms the presence of both of these dependencies and a control over the transition from one to the other is achievable. A threshold size limit for such a transition has been identified demonstrating that the dependency between drop size and its ve-

locity is not unidirectional. This thesis further explores the evaporation of double emulsion droplets and identifies two new regimes of evaporation. Resurfacing of a daughter droplet from an evanescing drop preceded by sudden spreading are uncommon observations in the literature. Detailed comprehension of the resurfacing of micro-droplets provides a possibility to control the evaporation mode, which was considered to be a random occurrence in the past.

Preface

This thesis is an original work by Muhammad Rizwanur Rahman. All works summarized in this dissertation are *my own* with the exception of Chapter 2, where the experiments were conducted by Haritha Naidu M. who was a visiting summer student at University of Alberta as part of the undergraduate research program and Bharath Kattemalalawadi. M.R.R. interpreted the data and wrote the manuscripts and P.W.R. revised the manuscript. I am completely familiar with all the steps involved in the experiments for their outright similarity with that employed for the studies reported in the other two chapters of this thesis where it was my sole responsibility to design and conduct the experiments, analyze the results, develop theoretical frameworks and to write the manuscripts. Dr. Prashant R. Waghmare supervised the research with conceptual formulation of the problems and by revising the manuscripts.

A version of Chapter 2 of this thesis has been submitted for possible publication in Langmuir as: Muhammad Rizwanur Rahman,Haritha Naidu M., Bharath Kattemalalawadi and Prashant R. Waghmare as: "Dynamics of Drop Spreading on Liquid-Fluid Interface". A version of Chapter 3 of this thesis has been published in Physical Review Fluids as: Muhammad Rizwanur Rahman and Prashant R. Waghmare, "Influence of outer medium viscosity on the motion of rolling droplets down

an incline", *Physical Review Fluids*, 2018, 3(2), 023601. A version of Chapter 4 of this thesis is currently in revision for publication in Soft Matter as: Muhammad Rizwanur Rahman and Prashant R. Waghmare, "Evaporation of double emulsion drop and resurfacing of daughter droplet".

Dedicated -

to my family:

Prof. A. K. M. Shafiqur Rahman and Prof. Razia Begum, my parents

M. Mushfiqur Rahman, my elder brother

and Toishy, our princess

- they animate my world.

To my grandfather (dada) - whom I never met but can feel in the flow through my veins. And to my grandfather (nana) and the three million martyrs of 1971 liberation war,

who kissed death for our right to live.

Acknowledgements

My sincere gratitude extends to Professor Dr. Prashant R. Waghmare, my supervisor, without whom this thesis would never have been possible. He envisioned the project promises and guided me with his insightful suggestions throughout the program. Most importantly, his encouragement for aiming at high above the sky, made a significant difference. I sincerely thank my examining committee : Professor Dr. Morris R. Flynn, Professor Dr. Andrew R. Martin and Professor Dr. Alexandra Komrakova for their invaluable time and effort in reviewing my thesis. I am grateful to Dr. Aleksey Baldygin for his support throughout the program in training me on different instruments and providing with helpful suggestion.

Sincere gratitude to Professor Dr. Howard A. Stone for his generous gesture in editing the article which constitutes Chapter 3 of this thesis. I acknowledge Professor Dr. Jaco Snoeijer for providing insightful comments in the construction of the article that makes Chapter 2 of this thesis. I acknowledge technical support from KR$\ddot{U}$SS GmbH and Media Cybernetics in instrumentation and data processing.

I would like to extend my special thanks to Dr. Shabbir Mustafiz and little Sophie - who never let me feel homesick; and to Ishita Biswas, Farhad Ismail, Abrar Ahmad, Ahsan Ullah and Mohammad Abu Hasan Khondoker for making my journey worth remembering. Thanks to Professor Dr. A.B.M. Toufique Hasan for his care in my undergraduate training at BUET that prepared me for my future voyage. Last, but not the least, I am indebted much to my lab members for their support and inspiration.

Contents

List of Tables

List of Figures

Chapter 1

Introduction

1.1 Thesis Outline and Scope

In contrast to the convention of focusing on a number of topics that eventually make a single string, I enjoyed the opportunity to work on three parallel projects in my Master's thesis. However, the projects are closely inter-related from the perspective that each of them investigates certain aspects of multiphase microfluids, in particular the fundamentals of double emulsion droplets. Motivated by the celebrated remark of Professor Richard Feynman that *there's plenty of room at the bottom*, when I investigated the rarely explored features of compound micro droplets, each of the projects revealed surprising physics. This allowed me to let the findings lead the research rather than pursuing a pre-defined matrix.

This thesis initially aimed to investigate two different but extremely important features of a compound droplet, (i) rolling dynamics of double emulsion droplets in a viscous medium that constitutes Chapter 3 and (ii) evaporation of double emulsion droplets that is described in Chapter 4 of this thesis. Each case revealed some unexpected observations that inspired us to compare the findings with the single phase counterpart. But the scarcity of the literature on those particular findings

necessitated the detail investigations of simple single phase droplets.

Generation of double-emulsion drop is one of the requirements to investigate the envisioned projects. Well established needle-less drop deposition technique is extended for the generation of double-emulsion drops. Appropriate selection of liquid combination and different operating parameters are crucial for such compound drop generation. So an impulse to look into the reasons for the experimental challenges and intricacy in the 'supposedly well predictable' generation became essential. This impelled us to study the short time dynamics of drop spreading on a liquid-fluid interface which constitutes Chapter 2 of this thesis.

In the effort of maintaining each chapter as a 'free standing' research, Chapters 2, 3 and 4 of this thesis contain elaborate introductions as they appear in the communications. Hence, this first chapter briefly addresses the problems investigated in Chapters $2-4$ and emphasizes on introductory discussion of the motivation of the research and background of double emulsion droplet, their applications and generation techniques followed by concise overview of each of the chapters.

1.2 Double-Emulsion Droplets

Multiphase microfluidics is a celebrated confluence in today's world where physics, chemistry, biology and engineering blend together [1]. It possesses enormous potential and promise in radicalizing numerous technologies and in ushering surprising simplicity in tackling problems that were otherwise believed to be complex and even impossible to deal with [2–13]. The study of multiphase droplets has been a burgeoning area of research due its wide range of applications [1, 14]. Interfacial characteristics at different phases dictate the successful generation of multiphase droplet in the miniaturize world. The complexity in identifying the role of different operating parameters for desired outcome relies on understanding of every interfacial activity. In this thesis entire attention is devoted mainly to double-emulsion droplets.

1.2.1 What is Double Emulsion Drop

Though the first work on multiphase drops can be traced a century back [15], the fundamental studies on the dynamics of encapsulated drop systems only appear no sooner than the 80s [16–18]. The so-called double or multiple emulsion drop system, also often termed as emulsion of emulsion, duplex emulsion, multiple emulsion or compund drops interchangeably [19], can be defined as a drop completely engulfed or encapsulated by another immiscible liquid drop [20]. Popularly being of two main types, *i.e.*, water-oil-water and oil-water-oil, a double drop system can contain multiple as many as hundreds of inner drops or only a few if not only a single inside the outer drop [14].

1.2.2 Double Emulsion Drop : Opportunities

The ability in simultaneous encapsulation of multi-components inside the fluid pocket has turned double emulsion drop system into a powerful tool in microfluidics technology. A high degree of control over the size or volume ratio of the associated phases in a double drop system promises much for encapsulation technology that finds its potential in drug delivery [3, 4, 6], food processing [5], bio-medical applications [7] and for selective mass transport [20].

Double emulsion drop system is of rapidly growing interest to the food scientists because of their promise in (i) preparing reduced fat emulsion products and (ii) protecting any sensitive or bioactive nutrient by encapsulation in order to release them in a timely fashion during eating or digestion [19]. It has found its promising applications in many different ways [19] such as, double emulsion containing polysaccharide [21], replacement of milk fat in cheese [22], spread enriched with fish oil [23], encapsulation of Lactobacillus delbrueckii [24], replacement of oil by water droplets in oil phase to manipulate sensory response [25] and many other applications [14, 19].

Double emulsion drop systems are ideal micro reactors [26] for their ability of encapsulating one acting reagent inside another non-reacting and immiscible liquid drop. In this context, applications that require screening of millions of separate reactions find their promise in such emulsion systems [2]. In particular, directed evolution methods [27] that are limited by the requirement of high throughput measurement of biochemical reactions, now find their potential in the promise of ultra-high screening ability in droplet based microfluidic technology [27].

Multiphase microfluidics can bring revolutionary improvements in targeted drug

delivery utilizing the potential of double-emulsion drop systems. While usual drug delivery methods (nasal or oral) fall short of stability and solubility in targeted delivery, encapsulation of the drug can easily overcome those limitations [14]. In cancer treatment, chemotherapeutic agents leave malign effects on the surrounding healthy cells and tissues. This severely limits the application of required amount of dose of the reagents to the cancer affected cells. A controlled targeted local delivery of the reacting agents can greatly amplify the amount of dosing while not affecting the surrounding healthy sites [28]. Double emulsion drop systems show enormous promise in improving the efficacy of cancer treatments by combining the benefits of stability as well as slow and prolonged release of the drugs to targeted sites [29]. Numerous anticancer, anti-inflammatory and antibiotic drugs are encapsulated by double emulsion technique [14].

Inertial confinement fusion (ICF), which requires controlled multilayer structure target for better ignition and detonation, can be significantly enriched and improved by utilizing the power of multi emulsion systems [30]. Fuel can be encapsulated as an inner drop inside an outer shell and then transported to the detonation site [31]. On-chip electric field actuated microfluidic assembly of double emulsion droplets [30, 31] can bring remarkable efficacy in achieving this high precision in controlling required volume ratio for successful ICF.

It is worthwhile to state that microfluidic technology is seeing much of its future in finding superior control on the generation, locomotion and stability of multiphase, *i.e.*, double emulsion drops. However, being a complex system of multiple interfaces, it offers much difficulties in terms of stability as compared to its single phase counterpart. Obtaining the appropriate combinations of inner and outer

phase fluids is a challenge. On top of that, processes that require precise deposition of such complex system without compromising any deformation and alteration due to kinetic energy, generation of such micro droplets brings additional difficulties. The next section briefly discusses the generation of such double drop system that has been developed in our research group.

1.2.3 Generation of Double Emulsion Drop

While the potential of double emulsion drop technologies demonstrates unprecedented improvements in microfluidics, its complex multiphase nature also brings numerous barriers from application perspective. Based on the application where it is being used, the requirements of accuracy and precision vary. However, from the broader point of view, generation, control and attainment of stability with desired dispersion offer the most difficulties. Among different methods of double emulsion droplet generation, some of the prominent techniques are listed in Table 1.1 based on their homogenizing principle [19].

Table 1.1: Methods of emulsification for generating double emulsion droplets

Stirrer technique [32]	Low pressure technique [33]
Rotorstator technique [34, 35]	Ultrasound technique [36, 37]
Membrane emulsification technique [38]	Micro channel technique [39]
Edge based droplet generation technique [40]	Spinning disk technique [41]
Single and double stage high pressure technique [42–45]	

The microfluidic technologies that can make improvements using the potential of double emulsion droplets, require precise volume and size control, desired dispersion and stability, and high encapsulation efficacy. However, each of the conventional methods listed in Table 1.1 fall short in full-filling one or the other of

these requirements. Our research group has addressed these difficulties and limitations of double emulsion drop generation and developed a new simple technique to generate such complex drop system with precision and accuracy (manuscript under preparation). Also large number of such compound drop system can be generated in isolation from one another which increases the degree of freedom in their successful applications. This method, established in our group provides the opportunity to generate double emulsion droplets for experiments with precision and accuracy which are of prime importance in numerous applications as well as for fundamental research of such system.

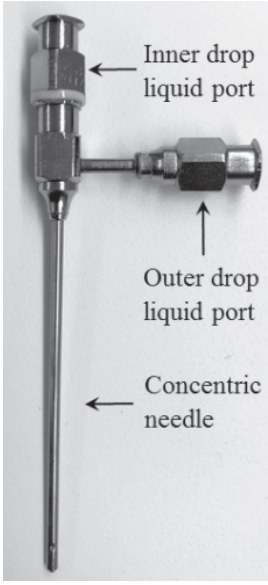

Figure 1.1: Generation of double emulsion drop using a concentric needle-pair (Custom coaxial needle, 100-10-coaxial, ramé-hart instrument co.)

In all the experiments described in this thesis, single phase droplets were generated as presented in Waghmare et al. [46]. Generation of a double emulsion droplet requires designing of a customized device as depicted in Fig. 1.1. This technique uses a concentric needle pair with two different inlets for pumping the fluids. With

a smaller diameter ($d_o = 0.5mm$), the inner needle is projected outside of the outer needle which has a larger diameter ($d_o = 1.8mm$). For the experiments reported in Chapter 3 and 4, the inner needle was connected with the deposition unit of DSA 100E (KR$\ddot{U}$SS GmbH) while a secondary pump was connected with the inlet port of the outer needle. First, the outer phase liquid was pumped through the outer drop inlet port (port *o*) with precise volume and a drop was generated with the inner needle projected inside the drop. Then the inner drop deposition unit of DSA 100E pumped the inner drop liquid at desired flow rate and volume to generate an inner drop inside the already generated outer drop. The generated double-emulsion drop at the tip of the co-axial needle is further impacted on a liquid-fluid interface to get the successful detachment of the double emulsion drop form the needle.

1.2.4 Interfacial Detachment

Although the generation of such a controlled double emulsion drop is always challenging but possible with a high level customized device, more challenge lies in its successful detachment from the needle without distortion in shape and size. However, this detachment process is not simple for even single phase droplets. A non-intrusive needle-less deposition method [46, 47] was deployed to achieve detachment without any shape distortion. Being substrate independent, this method enabled us to successfully deposit our single and double emulsion drop on the experimented substrates irrespective of their wettability. The detachment technique utilizes the difference of interfacial tensions of the associated fluids and imbalance of forces acting at the interface.

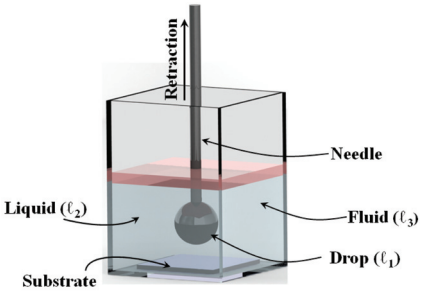

(a) Drop generation

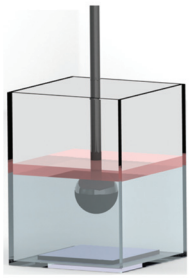

(b) Needle retraction

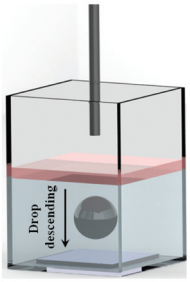

(c) Drop detachment

Figure 1.2: Needle less deposition of a single phase drop in a medium (a) first a drop is generated inside a liquid bath and a film is created at the interface (b) needle containing the drop at its tip is retracted through the film (c) as soon as the drop hits the liquid-film, it detaches and falls to the substrate underneath the bath (Adapted from Ref. [46] with permission of The Royal Society of Chemistry).

As shown in Fig. 1.2, a drop is first generated inside a liquid bath in a cuvette (Step I). Then a thin liquid lens is formed by dispersing an appropriate lighter liquid at the interface. After this step, the needle with the drop contained at its tip is pulled through the interface (Step II). As the drop hits the interface, it creates imbalance of interfacial forces and results in similar scenario as drop impact on liquid repellent surface. This facilitates the detachment of the drop from the needle. Careful selection of interface for lens does not permit the drop to spread on the interface. The selection of denser liquid compared to the liquid in the cuvette allows us to observe the fall of the drop in liquid bath. This idea of single phase drop deposition also

applies for a compound drop provided that all the liquids are carefully selected with appropriate interfacial tensions and densities.

As stipulated earlier, the successful detachment, however, is not very much trivial to occur in any liquid-fluid-drop combinations, rather requires careful selection of the liquids. Also, it is important to note here, all liquid-drop combinations do not require a lens for detachment. Instead, a liquid-air interface appear to be sufficient to detach the drop from the needle for certain combinations which can be easily explained by the Neumann triangle concept [48, 49]. Being a complicated phenomenon, this needle less deposition or detachment at the interface requires attention, careful consideration of different parameters and understanding the interfacial physics. The next section discusses this in greater detail.

1.3 Drop Spreading on a Liquid-Fluid Interface

Our research group exploited the energy imbalance at the interface to portrait the detachment technique to achieve an interfacial repellence and thus the needle less deposition of a drop [46]. In concise, in a situation where a needle containing a drop at its tip is pulled back through a liquid-fluid interface, there are two possibilities to occur. In one case, the liquid-fluid-drop combination satisfies the Neumann condition and attain equilibrium upon spreading on the interface. On the other hand, if the liquid-fluid-drop combination does not satisfy the Neumann condition, then there is energy imbalance at the interface. The drop-fluid and drop-liquid interaction and the liquid-fluid interaction alters the surface energy from the initial state. If energy is dissipated ($\Delta E < 0$) at the interface for this interactions, then spreading will be favored to minimize energy and to attain equilibrium. Whereas, the drop

will repel at the interface and fall back if the opposite is true ($\Delta E > 0$) [46].

For successful detachment, the downward push on the drop by the thin film or lens needs to be larger than the adhesion force between the needle and the drop. But in practice, when these forces are quite close, detachment is still possible utilizing the kinetic energy of the drop when it just hits the interface while the needle is retracted. In such cases, the drop doesn't get enough time to initiate spreading on the liquid-film interface, rather the interface repels the drop and thus assists in detachment. Opposite becomes true when the retraction speed is much slower than what is actually required. Our experimental observations suggest that, even if all criteria for successful detachment is fulfilled, detachment may not happen at all. Multiple trial-and-error attempts revealed that the role of the retraction speed cannot be ignored. In fact, when Neumann condition is not satisfied and detachment depends on the dissipation of energy, the competition between spreading time scale and that of the needle retraction plays an important role. If the retraction speed is much slower to allow the drop larger contact time than the spreading time scale, it will favor the spreading rather than detachment.

Any experimentation that requires successful detachment of the drop requires an understanding of the short time dynamics of spreading at liquid-fluid interface. The equilibrium state of a drop spreading at liquid-fluid interface or on a solid substrate is very well documented [50–58]. While the literature is rich in discussing numerous possible equilibrium configurations, to our surprise, it lacks in study on how a drop attains that well documented equilibrium condition on a liquid-fluid interface. This short time dynamics for a drop spreading on a solid substrate has been addressed [59–61] quite recently, but the spreading at a liquid-fluid interface scenario

remained ignored. But this turns out to be crucial when detachment at the interface is of prime interest. Hence, before proceeding with the exploration of double drop emulsion droplet dynamics, we studied the early time spreading phenomenon on a liquid-fluid interface to gain insight on the successful detachment. The physical understanding of such short time dynamics of drop spreading at liquid-fluid interface is also important in drug and food encapsulation and targeted delivery [3–5], oil recovery processes and bio-locomotion [62–64]. This study is reported in Chapter 2 in great detail. Understanding from this study allowed us to determine the appropriate time scale that facilitated successful detachment.

Our experience of detaching a single phase droplet with needle-less technique has been extended to the double emulsion drop scenario in light of the insight gained in the early time dynamics study in Chapter 2. The selection of appropriate retraction speed becomes more pronounced from the experimental point of view for a double emulsion drop system where the detachment offers higher level of complexity due to the addition of another liquid (inner drop) interacting with all the interfaces. While a handful of liquid combinations show successful detachment of the double-emulsion drop system from the liquid-fluid interface, complete theoretical development of the phenomenon is still underway in our group. While obtaining the double-emulsion drop, an interesting aspect was noticed. Irrespective of the surface energy of the solid substrate on which the double-emulsion drop was deposited, it never spread instantaneously. If the substrate is not perfectly flat, which is quiet common in most of the experimental cases, we observed a rolling of the deposited drops. This further enhanced our confidence and interest to quantify this rolling motion as opposed to the single phase droplet scenario. Interesting enough, thor-

ough literature review revealed that drop rolling on an incline in viscous medium is ignored and we attribute this towards the inability to generate the drop inside a liquid medium.

1.4 Drop Rolling in Viscous Medium

Creeping motion of a spherical body immersed in viscous fluids has always attracted scientists and researchers for detailed investigation. Stokes [65], in his pioneering study, discovered that a solid body, falling through a viscous liquid, decelerates quickly prior to attaining the steady terminal velocity. Numerous attempts have been made to investigate the role of different operating parameters while studying such motion in stagnant or moving fluids. In most of the cases, such studies are devoted to analyze rigid (solid sphere) body motion. When we refer to the classical work of Galileo (~ 1602) [66] discovering constant acceleration of such a body, a sharp contrast with the observations of Stokes cannot go unnoticed. This is because of the dissipation from the surrounding medium which becomes significant in Stokes flow but negligible in Galileo's situation. In Stokes flow [65], the resistance force from the surrounding medium results the fall with a diminishing acceleration until it reaches a zero acceleration and attains constant terminal velocity.

Contrary to Galileo's experiment, resistance from the medium becomes substantial in Stoke's flow. Thus the continuous diminishing acceleration and the attainment of steady velocity of descent can be attributed to this viscous resistance. In response to Stoke's observations detailed analysis was performed by numerous researchers to identify the role of surrounding media in case of rigid body motion [67–69]. Further, Saffman [70] suggested that a rotating and translating sphere

subjected to uniform shear experiences a lift force and a side force deflecting the sphere's trajetory. Prokunin [71] and Gohar [72] investigated the role of surface roughness and cavitation induced by Stoke's flow on the motion of a solid body moving under viscous medium whereas, in a detail analysis Bico et al. [73] reported the importance of sliding motion along with the rolling motion of a sphere coated with viscous layer moving on an incline. In such cases, the sphere size and density as well as the surface tension and thickness of the viscous layer present between the rolling body and the attached substrate affect the steady velocity of descent.

Though the discussion on the solid body motion has long been addressed, the recent development in microfluidic technology demands detail understanding of the dynamics of liquid drops in viscous medium for numerous applications [74–76]. With, the emergence of multiphase microfluidics, the understanding of the fundamental physics of such bodies has become more pronounced. However, with our effort in investigating the rolling dynamics of a double drop system by varying the volume ratio of the inner to the outer drop, the experiments seemed to exhibit quite unexpected and indecipherable results at first sight with almost no correlation among them. This highlighted our gap in understanding the single phase drop motion in a viscous medium. In the early 90s, scaling arguments of Mahadevan and Pomeau [77] predicted a surprising feature of a single phase droplet rolling on an incline in air medium. According to this argument, velocity of such a drop should decrease with the increase of its size and this was attributed to the increase in viscous dissipation at contact area for larger droplets. This claim was later experimentally proved by Richard and Quéré [78].

However, as we see in the historical development of physics (as from Galileo to Stoke) that consideration of a viscous medium significantly alters the outcome. Hence, we examined the scaling analysis [77] for a single phase drop rolling on an incline in a viscous medium. The theoretical development with this medium consideration resulted in emanation of a velocity behavior that is opposite from the literature [77, 78]. However, with increase in drop size, when we reached above a certain threshold, Mahadevan and Pomeau behavior was apparent. Thus our scaling arguments established one additional behavior and thus it allowed us to divide the rolling motion in two different regimes. Our experimental observations also suggested similarly as of our arguments for smaller drops below the threshold, but extreme difficulties were encountered to achieve drop size required to exhibit the inverse dependency between size and velocity of the drop. At this point, the results obtained from the double emulsion drop rolling experiments became clear, understandable and explainable. They clearly showed the existence of the two motion behaviors simultaneously only depending upon the volume ratio of the inner to outer drop. Also the arguments for single phase droplets could be easily extended to explain the double drop scenario. Chapter 3 of this thesis reports this study in great detail.

Finally, the natural extension of generation of double emulsion droplet in a liquid medium is to generate double-emulsion droplets in an air medium. The generation of double emulsion drop on a solid substrates in air medium was achieved with similar principle as followed for single phase or double phase drops in liquid medium. By serendipity, after allowing this compound drop to stay on the solid substrate, in an air medium, for a longer period of time, we observed quite an in-

teresting phenomena which we termed as resurfacing of daughter droplets. Hence, attention was devoted to the investigation of this phenomenon as the final study of this thesis.

1.5 Evaporation of Double Emulsion Drops

Droplet evaporation is crucial for numerous applications from DNA mapping [12] to chip manufacturing, inkjet printing, painting and coating technologies [13, 79, 80], self cleaning [81], bio-sensing [82] and droplet based micro-fluidics [83, 84]. The complex phenomenon has been well characterized for single phase droplet [85–90] and we extend the investigation for a double drop situation. The study of such evaporation or dissolution comes into necessity when we think about technologies fascilitating targeted encapsulated delivery of drug or active reagents [14, 29] where exposure of the protected inner drop is demanded at timely fashion. Understanding of the behavior of evaporation of the outer shell phase can provide a superior passive control on this time stamping. Apart from its application perspective, evaporation of sessile droplets (droplet resting on susbtaret is called as sessile droplets) has always been a topic of interest in fundamental and applied sciences [91]. We extended that investigation to double emulsion drop system and observed two new regimes in the evaporation spectrum, namely (i) 'transition' – where sudden spreading can be witnessed as the inner drop gets fully exposed after visible 'complete evaporation' of the outer drop and (ii) 'resurfacing' – where a daughter droplet is seen to regroup from a thin film with a noticeable jump in contact angle. Our experimentation with single phase droplets of the same liquids does not show the resurfacing on similar surfaces. A hypothesis was conceived to explain

this and based upon that, we exploited a single phase drop evaporation situation to achieve similar phenomenon.

Chapter 2 of this thesis reports the short time dynamics of viscous drop spreading at a liquid-fluid interface. Chapter 3 emphasizes on the influence of medium viscosity on the rolling motion of single and double emulsion droplets. Chapter 4 investigates the evaporation behavior of double emulsion droplets and identifies two new regimes of such evaporation.

Chapter 2

Drop Spreading on Liquid-Fluid Interface[1]

2.1 Introduction

The dynamics of droplet spreading on solid substrates is a classical moving boundary problem in fluid mechanics that has long been studied for complete and partial wetting scenario [50–56]. The interfacial and viscous forces determine the spreading rate of small viscous drops and this temporal evolution often follows Tanner's law [52, 92, 93]. In case of lower contcat angle case, the spreading of the bulk drop is indeed preceded by the progression of a pre-cursor that justifies the universality of the Tanner's law [94–96]. However, a wide range of variation in the exponents for this law can be attributed to the liquid and solid properties [49, 97–100] and wetting scenario such as partial [59] and electro-wetting [101].

Recently, the early time dynamics of drop spreading has attracted researchers for the knowledge being crucial for many microfluidics technology and its being a fundamental study in understanding the spreading time scale. Eddi et al.[61] observed that initial stage of spreading is independent of the contact line dissipation

[1] A version of this chapter has been submitted for possible publication in Langmuir as: Muhammad Rizwanur Rahman, Haritha Naidu M., Bharath Kattemalalawadi and Prashant R. Waghmare, "Dynamics of Drop Spreading on Liquid-Fluid Interface", (2018)

and wettabilitty. Importantly, very different dynamic law has been observed in the first steps of spreading before attaining the Tanner's law behviour [59–61]. The dissimilarity has been further manifested in the study of Carlson et al. [102] where the initial stage of viscous drop spreading is seen to follow a square root growth with dependency on the liquid viscosity.

It is needless to mention that characteristics of the interface, on which the droplet spreads, play vital role in governing the dynamics. For perfectly rigid and flat substrates, forces normal to the three phase contact line (TPCL) can be neglected. In such case, balancing the competing forces acting along the TPCL results in the classical Young's equqation [50]. However, in situations where the rigidity of the solid substrate is not significantly larger, the normal force component can deform the solid-liquid interface [103–105]. Therefore, in the case of liquid-fluid interface, the drop attains a lens form. Equilbrium configuration of this lens can be identified with Neumann's triangle [48, 49] and this transformation from Young's to Neumann's condition has been studied in detail by numerous authors [57, 58].

Though the spreading dynamics of small drops on solid substrates has been very well documented, surprisingly a limited attention is given on the dynamics of drop spreading on a completely depformable interface, *i.e.*, liquid-fluid interface. The physical understanding of such a phenomenon is important in numerous applicaitions, including but not limited to, drug and food encapsulation and targeted delivery [3–5], oil recovery processes, surface water proofing and biolocomotion [62–64]. A few studies have investigated the spreading on liquid-fluid interface mainly focused on the equilibrium configuration [106, 107]. The attainment of this equilibrium is fundamentally as rich as drop spreading on a solid or

soft substrate and it is worthwhile to study this dynamics. However, how a drop spreads on such a stretchable interface and how the spreading dynamics differ from its rigid interface counterpart remain unanswered till to date. More importantly the role of drop viscosity in dictating the early spreading of a drop on a flexible liquid-air interface has been ignored in the literature. This present study addresses these situations and concentrates on the early time dynamics.

2.2 Experimental Methods

A silicon oil droplet of $1.5 \pm 0.1\ \mu L$ was carefully generated inside a water bath in a cuvette and brought near a liquid-fluid (water-air) interface. The oil drop detached at the interface due to the appropriate interfacial tension and attempts to attain equilibrium configuration through a transient spreading process. This phenomenon was recorded at high frames per second that allowed us to observe any event occurring within one-fourth of a millisecond. Four different grades of silicon oil (Paragon Scientific Ltd. and Cargille Laboratories) were used to observe the effect of drop liquid viscosity on spreading. Properties of the considered liquids (from MSDS sheets provided by the suppliers and our laboratory measurements) are reported in Table 2.1. De-ionized water was used as the liquid medium in a controlled environment with its free surface as the water-air interface. Please refer to Ref. [108] for further experimental details. Each experimental case was repeated for atleast 3 times and corresponding deviation in the data is reported in appropriate sections.

Table 2.1: Liquid properties of spreading droplets

Drop liquid	Viscosity $(mPas)$	Surface tension (mN/m)	Density (g/cm^3)
D10	10.32	40.6	0.846
S60	100.6	40.4	0.857
Laser Liquid	197	24.2	1.064
D1000	990	40.6	0.870

2.3 Results and Discussion

Spreading starts immediately as the drop detaches from the needle at the interface. Within a few milliseconds contact angle reaches a minimum value and a precursor footing becomes visible. Unlike spreading on a rigid substrate, in case of spreading on a liquid fluid interface, the vertical interfacial force component on the three phase contact line assists the deformation of the underlying interface. At the same time, drop spreads along the horizontal direction. The competition between the horizontal and vertical force components results in the appearance of two angles, θ_c and θ_{cap}. These two angles as well as the drop height are schematically shown in Fig.2.1 (a). We will first discuss the spreading of viscous drops in section $2.3.1$ and then extend our discussion on the observations of inertial oscillation for a drop of lower viscosity in section $2.3.2$ of this article.

2.3.1 Viscous Drop Spreading

Figure 2.1 (b) shows snap shots of Regime (I) $-$ initial spreading with no visible precursor, Regime (II) $-$ appearance of precursor as well as cap angle and, Regime (III) $-$ merging of the two angles into one that approaches equilibrium. In this representation a silicon (S60) drop spreading on water-air interface is shown. These

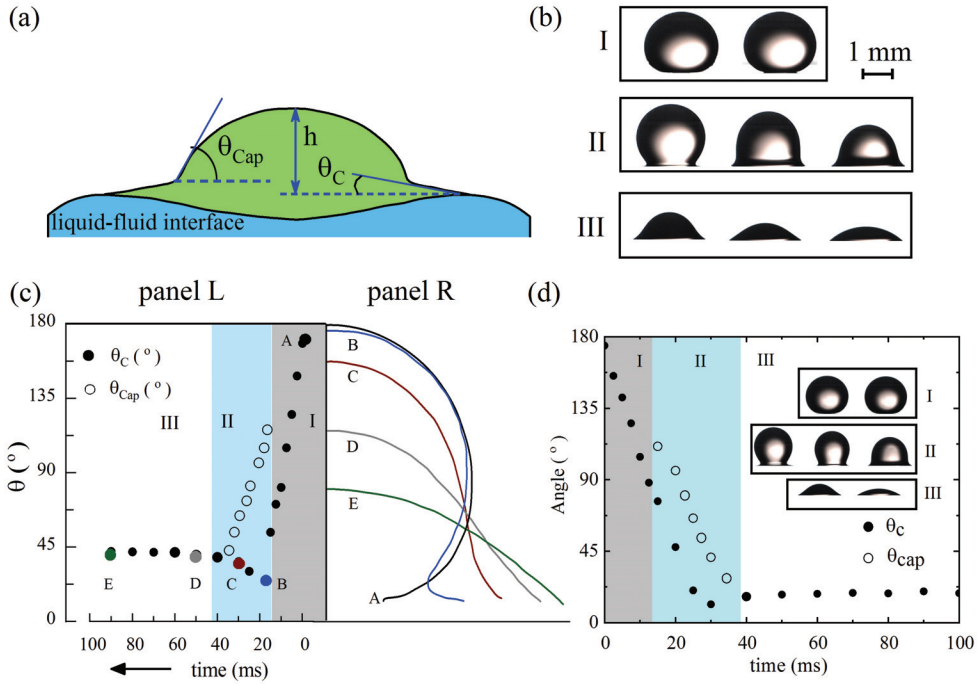

Figure 2.1: Transient spreading of a droplet on water-air interface: (a) Schematic diagram of the drop spreading with an underlying precursor footing which allows the definition of a two angles, cap angle θ_{cap} and contact angle θ_c (b) Different stages of silicon (S60) droplet spreading on the interface: (I) initial drop spreading, (II) emergence of precursor footing with two different angles, θ_c and θ_{cap}, (III) disappearance of the footing by the convergence of the two angles into one single contact angle (c) Drop profiles (A−E) depict the shape evolution and corresponding transient variations in θ_c and θ_{cap} (d) temporal variation of θ_c and θ_{cap} for a more viscous drop (laser liquid) with with three distinct stages of spreading in the inset.

three distinct regimes can be identified in Fig. 2.1 (c) where the temporal variation of the two angles are plotted for the same combination of drop-interface in Panel − L, whereas the corresponding drop profiles are presented in Panel − R. Initially (in Regime I), the interface behaves as if it repels the drop − similar to the observations in numerous study for drop spreading on solid substrate [109] and a near $180°$ contact angle can be observed for a while as seen at point A. Respective drop profile is (labeled as A in panel R) also depicts this scenario. The evolution of drop shape

can be witnessed from drop profiles A $-$ E. In Regime I, the contact angle rapidly decreases and at the end a large cap angle appears (B) in the beginning of Regime II. The cap angle θ_{cap} (shown by empty symbols in panel L) decreases fast while the contact angle θ_c, (shown by the filled symbols) starts to slightly increase. At the end of the Regime II, these two angles approach each other (at C) and in Regime III (at D), they converge into a single contact angle. Eventually the balance between the components of interfacial tensions results in lens formation with an equilibrium contact angle (at E). We find similar behavior for other liquids considered in this study and Fig. 2.1 (d) shows the spreading of laser liquid drop on water-air interface. The quantified analysis of contact angles as well as the drop shapes for varied combinations of drop viscosity is studied in detail to identify the spreading behavior as depicted in Fig. 2.2.

Figure 2.2 (a) $-$ (c) show the temporal variations in the quantified drop shape properties, *i.e.*, contact angle, θ_c, drop base radius r (non-dimensionalized by equilibrium radius, R_e) and drop height h (non-dimensionalized by initial drop diameter, $h_o = 2R_o$) for all the four different grades of Silicon oil. It is evident that increase in viscosity prolongs the spreading time. Also the spreading rate is much higher at early stage which slows down as spreading continues and approaches equilibrium. We observe an interesting oscillatory behavior in the spreading of a low viscous oil drop (D10) as seen in Fig. 2.2 which will be discussed in greater detail in the later part of this article.

It is a common notion to obtain scaling behavior to understand the universality in drop spreading [59, 93]. The abundance of solid substrate case studies motivates us to compare the spreading in light of a characteristic time. The short time dynam-

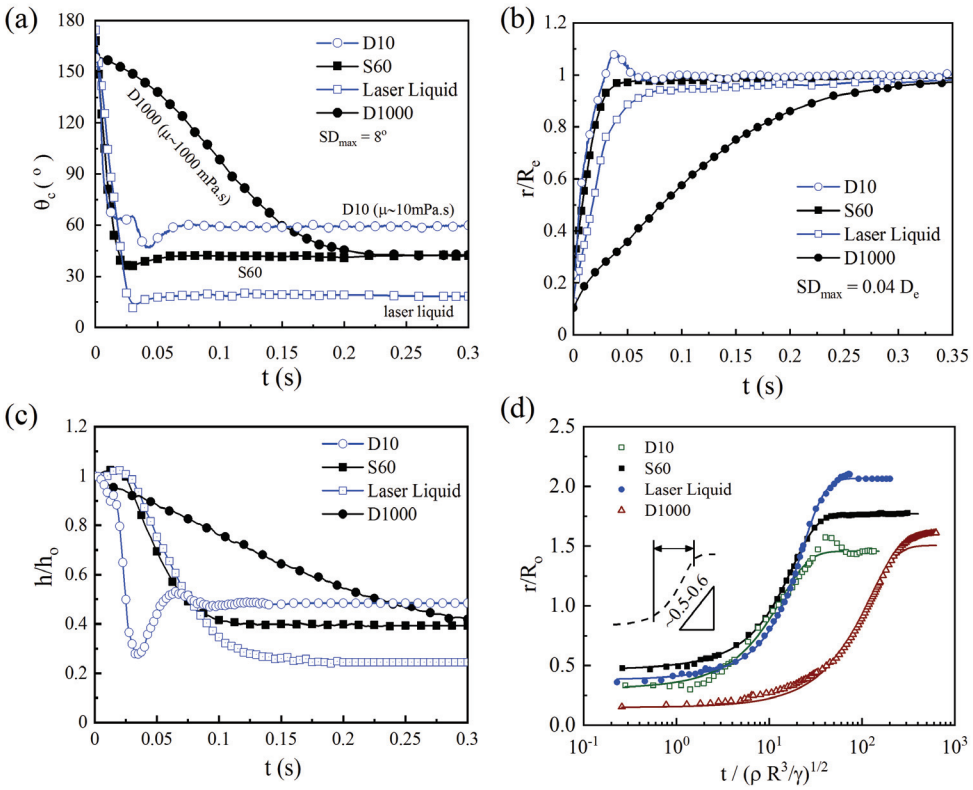

Figure 2.2: Temporal variation of (a) contact angle, θ_c (b) drop base radius (non-dimensionalized by initial drop radius) and (c) drop height (non-dimensionalized by initial drop height) for drops of different viscous liquids (d) spreading patterns of the drops suggest a power-law response.

ics in capillary regimes are mostly governed by the competition between inertial or Rayleigh time scale ($\tau_i = \sqrt{\rho r^3/\gamma}$) and viscous time scale ($\tau_v = \rho r^2/\mu$). In Fig. 2.2 (d), dimensionless drop base radius is plotted for each experimental case against dimensionless time (non-dimensionalized by the inertial time scale). Quite interestingly, similarities in the power-law response for drops spreading on solid substrate become apparent. We observed that Eq. 2.1, obtained by performing the curve fitting exercise, can excellently predict the spreading dynamics for the later part of the spreading.

$$\frac{r}{R_o} = k\left[1 - exp\left(\frac{-\beta t}{\tau_i}\right)\right] \tag{2.1}$$

here $k = R_e/R_o$, where R_o is initial drop radius and R_e corresponds to the equilibrium drop base radius.

According to this equation, in theory, one finds vanishing contact base radius ($r \to 0$) in the limit of $t \to 0$ and contact radius approaches the equilibrium state ($r \to R_e$) as $t \to \infty$. At the early stage of the spreading this equation fail to match the experimental results where the spreading behavior is different than the later part of the spreading as depicted in the inset of Fig. 2.2 (d). This corroborates the possibility of a shorter-time spreading mechanism [59]. The inset of Fg. 2.2 (d), shows linear increase in base radius with time and soon this linear behavior transforms into power law dynamics. One can safely assume that the majority of the spreading behavior can be predicted by Eq. 2.1 which constitutes only one unknown $-$ a time constant β. Since the viscosity is the only property that is distinctly different for each cases, this constant can be attributed as a representation of the viscous time scale. Interestingly, this time constant shows a linear relation with viscous time scale, except for the case of D10 which is a very low viscosity liquid. Despite of the seemingly promising aspect of this linear dependency between viscous time scale, τ_v and time constant, β, we prefer not to generalize this due to the inadequacy of wide ranges of viscosity but it may interests researchers for detail investigation.

It is evident that the temporal response of base radius does not show a pure power law. Rather, a logarithmic response is noticeable, pointing to the slow transient variation of the exponent. Similar varying exponent spreading behavior was

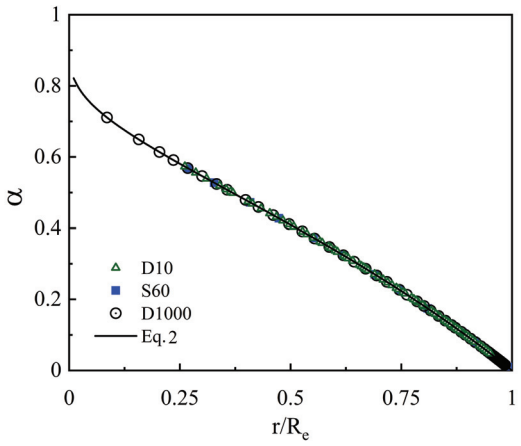

Figure 2.3: Evolution of apparent exponent α with non-dimensional drop base radius show excellent agreement between Eq.2.2 and experimental results

reported in Ref. [61] where Eddi et al. highlighted this slow variation by defining the exponent α as:

$$\alpha = \frac{ln(r/R)}{ln(r/R) - 1} \tag{2.2}$$

The unqiue way of this redefinition of α [61] takes care of the local variation of the exponent. In Fig. 2.3, we see excellent agreement between our experimental results and the prediction from Eq. 2.2. With this reprenstation of local variations of the exponent, Eddi et al. [61] suggested that the coalescence of two viscous drops and spreading of a drop on solid substrate are governed by same scaling arguments. Thus the solid substrate or the wall has no significance in the spreading dynamics. Though the validity of this analogy was argued for solid substrates, Fig. 2.3 confirms that in case of deformable liquid-fluid interface similar argument is plausible. This can be justified by assuming the studied spreading behavior to be similar to the drop coalescence behaviour where one drop is with infinite radius of curvature. It is worthwhile to state that the law for liquid drop coalescence well predicts the short

time dynamics of a drop spreading on a liquid-fluid interface. Also, one can see the collapse of all the four cases studied here onto a single master curve eliminating the effect of viscosity and signifying the intital geometry of the drop which resembels the observations for drop sprerading on a solid substrates [61].

2.3.2 Inertial oscillation in spreading

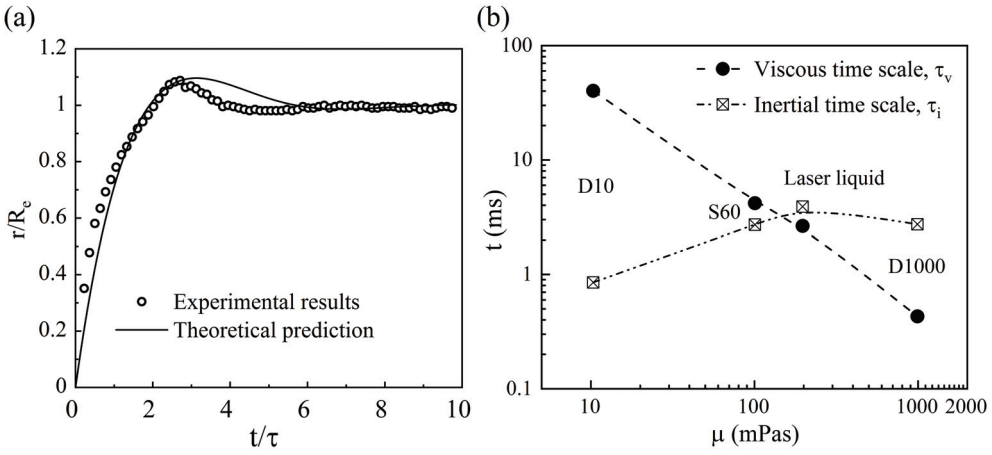

Figure 2.4: Inertial drop spreading on liquid-fluid interface (a) comparison of oscillations in base diameter observed for lower viscous silicon oil (D10) droplet with theoretical model (b) inertial and viscous time scales for the considered liquid drops

As mentioned earlier, for D10 oil drop, the contact angle, drop base diameter and drop height – all these three geometric parameters overreach their bounding limit and return to equilibrium as seen in the form of oscillation in Fig. 2.2. The base diameter and contact angle attain maximum and minimum limit respectively, and approach equilibrium with damped oscillations. The oscillation in base radius (Fig. 2.2 (c)) might be an interesting aspect that is different from the solid substrate spreading scenario. Most of the cases, the drop spreading on a solid-air interface is an irreversible process with a slip-boundary condition. Generally, the non-uniformity at the solid interface and the subsequent pinning at the three phase

contact line restrict similar oscillatory motion at the contact line and thus the oscillatory motion in the contact line. We attribute this difference to the the slip at the three phase contact line on the liquid-fluid interface. Repeated experiments showed similar behavior confirming the existence of such oscillation in spreading of low viscous fluids. The observation of this inertial oscillation though interesting, however, is not unexpected and reminds us of the studies on interial capillarity [110–112] where similar oscillation was observed for very low viscous liquids. Such oscillatory motions are governed by the nonodimensional equation as follows [110]:

$$\left(\frac{dr^*}{dt^*}\right)^2 + r^*\frac{d^2r^*}{dt^{*2}} + r^*\left(1 + C\frac{dr^*}{dt^*}\right) = 1 \tag{2.3}$$

here, the characteristic length for the radius was the maximum spreading radius. It is purposefully followed to pinpoint the overspread compared to the equilibrium configuration. Whereas, the time is normalized by the combination of characteristic drop spreading velocity and the initial drop radius. The tuning parameter, C is a non-dimensional damping parameter that varies proportionately with liquid properties and sensitive towards the viscosity. We find good agreement, as seen in Fig. 2.4 (a), between the prediction from this equation (Eq. 2.3) with $C = 1.05$ and the observations from D10 drop oscillations. The absence of such oscillations in the other three cases can also be predicted by varying the values of C where the oscillations are over damped. This can also be explained by comparing the inertial and viscous time scales and from Fig. 2.4 (b) where these two time scales are reported for considered silicon oil drops. It is evident that, for low viscous D10 drop, the inertial timescale is much smaller (at least by an order of magnitude) than the viscous time scale ($\tau_v/\tau_i \sim 50$) [113, 111]. With increase in viscosity, the viscous time scale becomes smaller and the ratio between these two time scales decreases and goes

below unity, i.e., ($\tau_v/\tau_i \sim 0.15$ for D1000) indicating an over damped situation, *i.e.*, oscillations are damped before their development. A special attention is required to identify the different spreading behaviors dominant by inertial, viscous or combined effects. The unavailability of liquids of viscosity lower than D10, with appropriate interfacial and physical properties restricted us to present the analysis for only one case but the detailed analysis with multiple combinations is warranted.

2.4 Conclusion

The short time dynamics of drop spreading on a liquid fluid interface exhibits similar behavior as that of the rigid wall case. This suggests the independent nature of the early spreading dynamics from the interface characteristics. A logarithmic response, instead of a classical power law, was observed which suggests a coalescence like behavior in spreading on a liquid-fluid interface. The similarity with coalescence raises the question on the influence of the curvature of the interface on which the drop spreads. In this particular study, the interface might behave as another drop with infinite radius of curvature and thus possibly qualifying the similarity. Low viscosity liquid drop spreading suggests that detailed attention is required for low viscosity liquids where prior to attaining equilibrium, oscillations in the drop shapes are inevitable.

Chapter 3

Rolling Dynamics in Viscous Medium[1]

3.1 Introduction

In the study of deformable body motion in a viscous medium, the dynamics become complicated due to dissipation from fluid motion inside and outside the body. In contrast to the case of a rolling non-deforming sphere, shape deformation, interfacial interactions (interfacial tensions and/or wettability) as well as contact line dissipation cannot be ignored in case of a rolling deformable body, such as a liquid drop. With recent advancement in micro-fluidics and an upsurge in the use of micro/nano fabrication techniques for numerous applications [74–76], the motion of droplets on solid surfaces in viscous media demand a thorough understanding. For example, it remains debatable [78] whether a liquid drop rolls or slides along a solid surface, particularly for low energy surfaces with very low roll-off angle. A defined criterion that demarcates these two types of motion is difficult to establish; in fact, an overlap between them has been witnessed during the transition from rolling to sliding motion [114, 115]. Mahadevan and Pomeau [77] discovered that,

[1] A version of this chapter has been published in Physical Review Fluids (PRF) as: Muhammad Rizwanur Rahman and Prashant R. Waghmare, "Influence of outer medium viscosity on the motion of rolling droplets down an incline", *Physical Review Fluids*, 2018, 3(2), 023601

unlike solid spheres, the velocity of a rolling liquid drop in air varies inversely with drop size. In this case, viscous dissipation at the contact area constitutes a form of resistance that varies based on the drop radius. This results in the inverse relation between drop size and its traveling velocity. For small droplets, inertia and viscous dissipation compete to dictate the outcome and in most cases the latter dominates the physics of the flow [77]. Richard and Quéré [78] experimentally verified this claim provided the drops maintain quasi-static shape [116, 77].

While the importance of medium viscosity is well established for cases of solid body motion [65, 68–71, 73], the role of the medium viscosity is ignored in most of the deformable body motion experiments. Griggs et al. [117] numerically and experimentally studied the motion of deformable drops sliding on an incline and paid particular attention to the role of the viscous medium. The authors discussed the possibility of the existence of two speed regimes. However, in most of the cases they analyzed, the drop size was beyond the capillary length scale limit resulting in sliding motion. Experimental evidence of the two rolling regimes, supported by a unified scaling argument, is still missing from the literature.

In order to fill this gap in the literature, we turned our attention to the role of the surrounding medium viscosity on the motion of liquid droplets on an incline. This exercise allows us to observe two distinct regimes (we will denote these two regimes as Regime I and II) for size-dependent velocity and comment on the parameters that demarcate the two speed regimes and therefore identifying the boundary between them. While our experimentation with single phase liquid drops confirms Regime I behavior and support the scaling model developed in this study, the exploration of Regime II required us to alter the experimental domain by using a double emulsion

drop to overcome the difficulties associated with a single phase drop rolling in this regime.

3.2 Experimental Methods

The experiment included the deposition of a drop on a glass substrate immersed in a viscous medium using a needleless deposition technique [46]. A schematic of the experimental setup is shown in Fig. 1(a). Droplet motion was triggered by precisely inclining the arrangement to an inclination angle (α). The drop's trajectory−from the deposited location to a point well beyond the point where it has reached terminal velocity−was recorded for further analysis. Since needleless drop deposition is a substrate independent method, we can avoid any unwarranted effects such as deformation of the droplet during deposition [46, 118, 47]. To investigate the role of medium viscosity on the drop trajectory, different combinations of drops and media (as presented in Table 3.1) were selected. To achieve certain drop-to-medium viscosity ratios ($\mu_R = \mu_d/\mu_m$), water (1000 kg/m^3, 1 $mPa.s$ with 0.01% Tween-20 solution), anhydrous alcohol (790 kg/m^3, 1.1 $mPa.s$), canola oil (920 kg/m^3, 72 $mPa.s$) and methanol (792 kg/m^3, 0.59 $mPa.s$) were used as surrounding medium. Microscopic glass slides were used as the substrates. The combinations were selected to achieve a wide spectrum of drop-to-liquid viscosity ratios (μ_R).

Table 3.1: Liquid properties of rolling droplets

Liquid	Interfacial tension (mN/m)	Density (g/cm^3)	Viscosity $(mPa.s)$
Silicon oils(two different liquids)	24	0.85 &1.06	10 &110
Glycerol water mixture(50-50, %v)	40	1.13	8
Paraffin oil	30	0.868	122.7

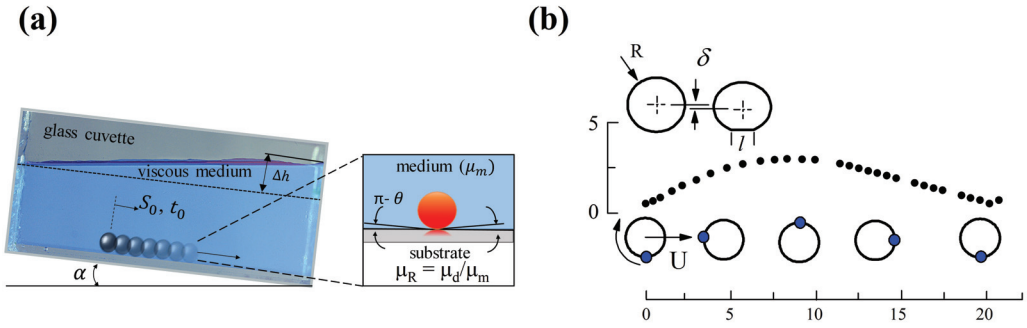

Figure 3.1: Under liquid rolling of single-phase droplet(a) Schematic of the experimental setup for observing the droplet motion along an inclined plane (not to scale). Snapshots of the moving droplet along its trajectory parallel to the bottom plane of the cuvette are provided, which were used to perform our analysis. The effect of the difference in the liquid reservoir level, denoted as Δh, is ignored in this analysis. The inset shows the instantaneous contact angle (θ) of the drop during its motion. The observed motion is assumed to be a rolling motion for very low contact angle hysteresis ($\Delta\theta \leq 7^{\circ}$) and high contact angle of the non-wetting drop [78]. (b) The lowering of the drop's center of mass due to its weight has been denoted by δ as shown in the schematic [77]. As a drop moves forward, we tracked a small marker on the drop which exhibits cycloidal trajectory. The schematic presented below the experimental data further depicts the motion of the marker as the drop rolls; the linear motion of the center of mass of the drop is denoted by U, the straight arrow indicates the direction of this velocity (U) and the curved arrow shows the direction of the droplet's rotation.

To achieve a double-emulsion droplet in order to explore Regime II behavior, a coaxial needle with two different sources of liquids was used. First an outer droplet was generated inside the viscous medium and later the inner needle slowly generated another droplet inside the outer one. By inserting a denser liquid droplet into the outer drop, a double drop was achieved, which is commonly known as a double emulsion drop [119, 120]. This double drop was then deposited using the needleless deposition technique. The rest of the experiments were carried out in the same way as single phase drop experiments.

3.3 Results and Discussion

3.3.1 Single phase drop rolling under viscous medium

To differentiate the sliding and rolling motion of the droplet, a marker along the periphery of the droplet (small air bubble with a drop) was introduced and the motion of this marker was tracked, as seen in Fig. 3.1(b). The cycloidal trajectory of the marker demonstrates the rolling mode of motion. The droplet rolls as it moves on the incline with a center of mass velocity U and in a very short time steady linear velocity is attained. In Fig. 3.2(a) the displacement shows a power law dependency on time $\sim t$ as reported for glycerol drop descent (in air [78]) and metal ball descent (on an incline lubricated with a thin viscous film [73]). For a glycerol drop rolling in air medium, inverse dependency between the size of the drop and descent velocity was observed [78], whereas with a viscous medium, the dependency changes as seen in the top-left inset of Fig. 3.2(a). For a liquid drop rolling in air, inverse dependency between size and velocity was attributed to the viscous dissipation at the contact area [78, 77]. But in the presence of a viscous medium, we observed that velocity increased with increasing drop size. Further, the bottom right inset of Fig. 3.2(a) suggests that medium viscosity alters the magnitude of descent velocity.

In a non-wetting case, if the contact angle is close to $180°$, a droplet of radius R can maintain a quasi-spherical shape forming a disk-shaped finite contact zone [77]. Most of the viscous dissipation occurs near the contact area besides that occurring within the drop. One can balance the rate of change of gravitational potential energy with viscous dissipation at the contact zone (which scales as $\sim \mu_d \frac{U^2}{R^2} \ell^3$ [77]), as well as an additional Stokes dissipation due to the presence of the sur-

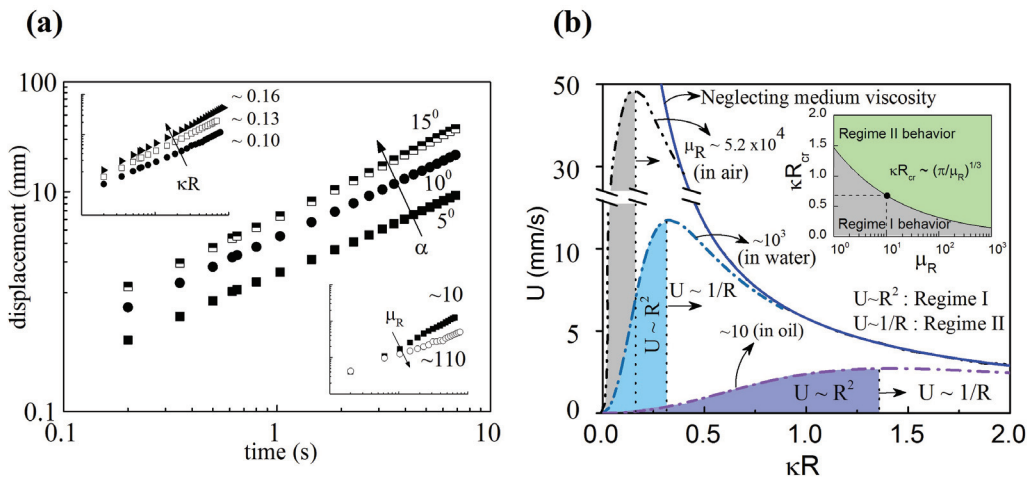

Figure 3.2: (a) Droplet trajectory at different inclination angles show weak dependency of the rate of displacement (velocity) on the angle of inclination. Top-left inset shows the displacement for varying drop size (κR) and bottom-right inset depicts the role of medium viscosity at the same inclination angle of $5°$(both the insets are presented for displacement versus time with same axes limits as figure a). (b) Theoretical prediction for droplet velocity is plotted over nondimensional drop size κR, where $1/\kappa$ is the capillary length and R is drop radius (typically less than 1 mm). Mahadevan and Pomeau model [77] (solid line) ignores the medium viscosity, whereas, the present model (dashed lines) accounts for resistance from the medium. Three different cases with μ_R of the order of $10, \sim 10^3$ and 10^4 demonstrate the role of medium viscosity. A viscous medium results in a regime (shaded region) where increase in size results in increase in the velocity. In the inset, progression of a critical or crossover length scale (κR_{cr}) towards higher drop size is observed as viscosity ratio decreases - this crossover size demarcates between the two velocity behaviors of the drop for a specific drop-to-medium viscosity ratio as shown by the dashed lines.

rounding viscous medium. This dissipation amounts to $\sim 6\pi\mu_m RU^2$. Here, μ_d and μ_m are drop and medium viscosity respectively and ℓ is the contact length that scales as $\sim \sqrt{(R\delta)}$; δ being the lowering of the center of mass of the droplet due to the slight deformation of the drop near the contact zone. These two are the major contributing forces to equilibrate the motion and the experimental results (presented in Fig. 3.3) suggest the same. Hence, in the presented scenario, we can justifiably ignore any rotational viscous dissipation due to the relative motion between the in-

terfaces. Further, as the drop moves along the surface, there might be an additional resistive force near the wall, in the neighborhood of the contact area, that is different from the bulk dissipation. If this force is disregarded, the scaling argument we present here remains unaffected and indeed predicts the obtained experimental data that will be discussed later in this article. Balancing the major contributing forces, one can obtain the following expression for drop velocity:

$$U \sim \frac{Bo\,\sigma sin\alpha}{\mu_d Bo^{3/2} + 6\pi\mu_m} \tag{3.1}$$

Here, σ is the interfacial tension of the drop in the considered medium and Bond number ($Bo = gR^2\Delta\rho/\sigma$). In this study, we present our results and arguments based on the characteristic length scale, κR ($= Bo^{1/2}$), where $1/\kappa$ is the capillary length. A similar expression as Eq. 1, with different pre-factor, can also be obtained by considering the dissipation in the lubrication region (the thin film region between the drop and the wall) [14, 22] instead of the bulk dissipation. The asymptotic solutions of the Stokes equations for a sphere rotating (ω) and translating (U) near a wall, bounding a viscous fluid with gap thickness ϵ $(\rightarrow 0)$, give the dissipation in lubrication region as $\sim R\,ln\frac{R}{\epsilon}\mu_m(U-\omega R)U$. Denoting the $R\,ln\frac{R}{\epsilon}$ and $(U-\omega R)U$ terms as R' and U'^2, one can obtain identical scaling behavior ($\sim \mu_m R'U'^2$) as of the bulk dissipation which is considered in this study. The bulk dissipation term in Eq. (3.1) becomes insignificant for a medium with negligible viscosity and results in a similar expression as proposed by Mahadevan and Pomeau [77]. Considering the effect of the medium, one can express drop velocity in terms of effective viscosity (μ_{eff}) as follows:

$$U \sim \frac{\sigma sin\alpha}{\mu_{eff} Bo^{1/2}} \tag{3.2}$$

where, $\mu_{eff} = \mu_d + 6\pi\mu_m/Bo^{3/2}$. A comparison between these two models (with and without considering medium viscosity) is presented in Fig. 3.2 (b). In contrast to Mahadevan and Pomeau [77] (Regime II), emanation of another regime (Regime I)−where velocity increases with size − appears only if viscosity of the medium is considered. With these two regimes, it is evident that the velocity of a descending drop can either increase or decrease with an increase in drop size. The shaded areas of the curves in Fig. 3.2 (b) schematically identify this Regime I where velocity increases with increasing drop size. Similar non-monotonic behavior (increasing and decreasing) for a creeping motion of non-spherical droplet sliding at a large inclination has been reported in the literature [121, 117]. Hodges et al. [114] theoretically investigated a number of regimes of velocity behavior that depended upon slipping, sliding or rolling mode of motion along with the shape of the liquid droplet. Their asymptotic theory for a rolling three dimensional drop suggests similar Regime I behavior. However, a distinct identification of the two regimes with experimental evidence is missing in the literature.

Fig. 3.2(b) shows that the contrasting velocity behaviors can coexist simultaneously for a wide range of viscosity ratio. In this figure, for each case, a crossover point is observed where the corresponding droplet becomes large enough to dictate the rolling motion merely by the viscous dissipation at the contact area. The drop experiences two dissipative powers acting against its motion. Balancing these two resistive forces gives a critical/crossover length scale $(\kappa R) \sim (\pi/\mu_R)^{1/3}$ that determines the boundary between the two regimes. We will denote this limiting size as

κR_{cr}. This divides the domain into two regimes which will be termed as Regime I (velocity increases with increase in size) and Regime II (velocity decreases with increase in size) in this article. Inset of Fig. 3.2(b) shows how the critical/crossover length scale progresses towards larger drops as viscosity ratio decreases. For example, a viscosity ratio of ~ 100 (as shown by the dotted lines in the plot) would results in a critical length scale of ~ 0.65. A drop below this dimension would travel with regime I behavior and a larger drop would exhibit regime II behavior. It can be noted here that for very high viscosity ratios, the critical length scale tends towards sticking thresholds [78] and for very low viscosity ratios, this length scale exceeds experimental limits.

The two regimes can be investigated for a given inclination by considering two limiting cases, *i.e.,* negligible and comparable viscosity of the medium. When medium viscosity is negligible, μ_{eff} becomes comparable to μ_d and $U \propto 1/Bo^{1/2}$ (*i.e.* $U \propto 1/R$). On the other hand, for a viscous medium the resistive components assure the coexistence of the two regimes. Theoretically, when a droplet rolls in a medium with negligible viscosity, it can experience both regimes, as shown in Fig. 3.2 (b) by the dashed line (with $\mu_R \sim 5.2 \times 10^4$). If the drop is small enough ($< \kappa R_{cr}$), it can demonstrate Regime I behavior, i.e., $U \propto R^2$, but the realistic magnitude for a given liquid drop in air is practically impossible to achieve where the sticking threshold is difficult to surpass [78]. For example, in the case of a glycerol drop in air, this critical radius threshold results in $\sim 200\mu m$. Such a small drop size is almost impossible to deposit without any external kinetic energy implications. More importantly, even if a successful deposition for rolling is achieved, the contact area where the dissipation dominates the sticking thresh-

old [78] may not permit the drop to roll [122]. These practical limitations restricted the researchers to perform experiments that can reveal the existence of regime I. In commonly studied cases, the contact base radius increases sharply with the increase in drop size and thus invites dissipation with a greater exponent of drop size ($\propto R^4$) compared to the gravitational driving force ($\propto R^3$). Subsequently, a drop asymptotically tends to attain lower velocities as its size grows [77, 78]. In Fig. 3.2 (b), the solid line depicts the velocity variation predicted by the model presented in the literature (Regime II) [77] while the dashed lines (with $\mu_R \sim 5 \times 10^4$) represent both Regime I and II predicted by the model presented in this study. Both models agree with each other above the crossover size (κR_{cr}) but there is disagreement below this threshold, which becomes more pronounced in the presence of a viscous medium as demonstrated for cases using water $(\mu_R \sim 10^3)$ and oil $(\mu_R \sim 10)$ media.

Regime I, which is difficult to achieve in a medium with negligible viscosity (*i.e.,* air), can easily be demonstrated by altering the medium viscosity. With a viscous medium scenario, the smaller droplet size results in point contact as opposed to the finite contact length during the droplet descent which makes the dissipation at the contact area almost negligible compared to the gravitational driving force and bulk dissipation from the surrounding medium. The displaced center of gravity (by an amount δ, as shown in Fig. 3.1 (b)) of the rolling droplet, due to it's own weight, becomes significantly above κR_{cr} where all three forces have same order of magnitude and hence transition to Regime II can be noticed. Since the contact length ℓ scales as $\sim \sqrt{R\delta}$, the contact area can be regarded as a point contact for drops with size less than κR_{cr}. As we increase the medium viscosity dominance (or decrease drop to medium viscosity ratio), Regime I operating zone can be maneu-

vered. As observed in Fig. 3.2 (b), if medium viscosity is magnified by two orders, the operating range for drop size in Regime I widens significantly. However, the experimental domain is constricted by several factors. Besides the sticking thresholds and creeping flow assumptions, the needle-less deposition technique imposes further limitations in selecting the liquid combinations. Additionally, the necessity of immiscibility and inert nature between the drop and medium is paramount. With these restrictions in mind, the combinations of drop and medium liquids are selected for investigating Regime I in a detailed manner.

In Fig. 3.3 (a) and (b), steady state drop velocities for viscosity ratio ~ 110 and ~ 0.1 are presented against κR at different inclinations. The dashed lines are the velocity predictions by equation (3.1) and symbols represent the corresponding experimental outcome. To account for the geometric constants in the scaling analysis, an appropriate empirical coefficient has been added to the theoretical prediction as a multiplying factor, i.e., $U_{exp} = k \times U_{th}$ (where, $k = \pi/3$). One can normalize the velocity as Capillary number ($Ca = \mu U/\sigma$) where viscosity can be of either the medium or the drop. To pinpoint the importance of the medium viscosity, Ca in Fig. 3.3 (c) is defined with medium viscosity. Our results show excellent qualitative agreement with the proposed scaling analysis and therefore we suggest that our experiment allowed us to explore regime I for the rolling drop motion. For $\mu_R \sim 110$, as drop size increases by a factor of ~ 1.5 (κR from 0.05 to 0.08), velocity increases by a factor of ~ 4. Further increase in drop size by the same factor (~ 1.5) results in merely a ~ 2.9 times increment in velocity. Thus velocity experiences a diminishing increment as drop size increases and will reach a maximum magnitude at κR_{cr}, prior to beginning to exhibit Regime II behavior.

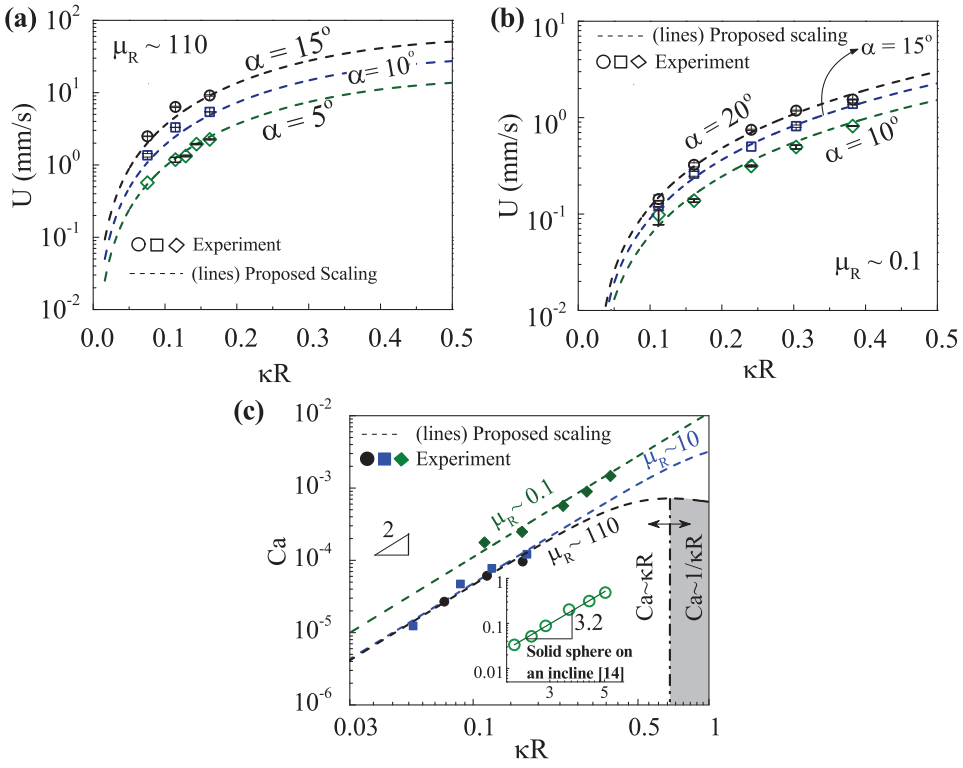

Figure 3.3: Droplet motion for Regime I under different operating parameters: (a) Silicon-oil drop rolling in water medium, $\mu_R \sim 110$, at different inclination angles (open diamond– $\alpha = 5°$, open rectangle– $10°$ and open circle– $15°$) (b) water-glycerol drop rolling in canola oil medium, $\mu_R \sim 0.10$, (open diamond– $\alpha = 10°$, open rectangle– $15°$ and open circle– $20°$). Maximum error obtained for experiment is $\pm 8\%$ (c) Non-dimensional descent velocity of liquid droplets increases with κR in Regime I for different drop-medium combinations. Inset (reconstructed from experimental observations of Bico et al. [73]) shows power law dependency between the two parameters for a non-deformable body.

In Regime I, the deformation of the contact area and hence the associated dissipation can be ignored. It allows us to observe an increasing trend that is compatible with intuitions for a rigid body. This reminds us the work of Bico et al.[73], where the authors studied the motion of a rolling sphere on an incline lubricated with a thin viscous film. The motion of a rigid body down an incline exhibits a stronger power law dependency (3.2 ± 0.05) as seen in the inset of Fig. 3.3(c). The difference in the power law between the two cases (deformable drop and rigid body

descent) is another aspect that we would like to bring to the reader's attention. The presence of an outer viscous medium along the entire interface of the drop, as opposed to thin film at the contact area may be the cause of the nonconformity of the exponents. However, the present soft body study being very different from the rigid body motion, this comparison is tentative only.

3.3.2 Double emulsion drop rolling under viscous medium

In order to extend our analysis of liquid drops to witness Regime II behavior in a viscous medium, κR needs to be significantly larger. For example, with $\mu_r \sim 100$, κR should be ≥ 0.65, which results in a drop diameter of $\sim$ 5mm. Achieving a drop of this radius is restricted by the spherical shape assumption. In this case, to retain a spherical shape, a drop radius must be smaller than ~ 1.9 mm; larger drops undergo too much deformation. For highly viscous medium (*i.e.*, $\mu_R \sim 0.1$) this size is too big to attain. On the other hand in a medium with low viscosity, (*i.e.*, $\mu_R \sim 10^4$) the drop size is too small to avoid the sticking threshold. These limitations impede us from performing the experimental analysis with the considered combinations of drop and medium. Therefore, we have carefully engineered the experiments to overcome this barrier so that we might still observe Regime II. If κR of the drop can be increased above κR_{cr} without altering the drop size (so that its spherical shape is not deformed), exploration of Regime II becomes easier. The apparent dilemma between size and deformation can be easily solved by instilling a denser and immiscible liquid drop inside the rolling drop. This allows us to observe the rolling of a double emulsion drop consisting of both inner and outer drop phases. This not only facilitates the demonstration of the contrasting velocity behaviors,

also it widens the degree of freedom for the selection of liquids for experimentation.

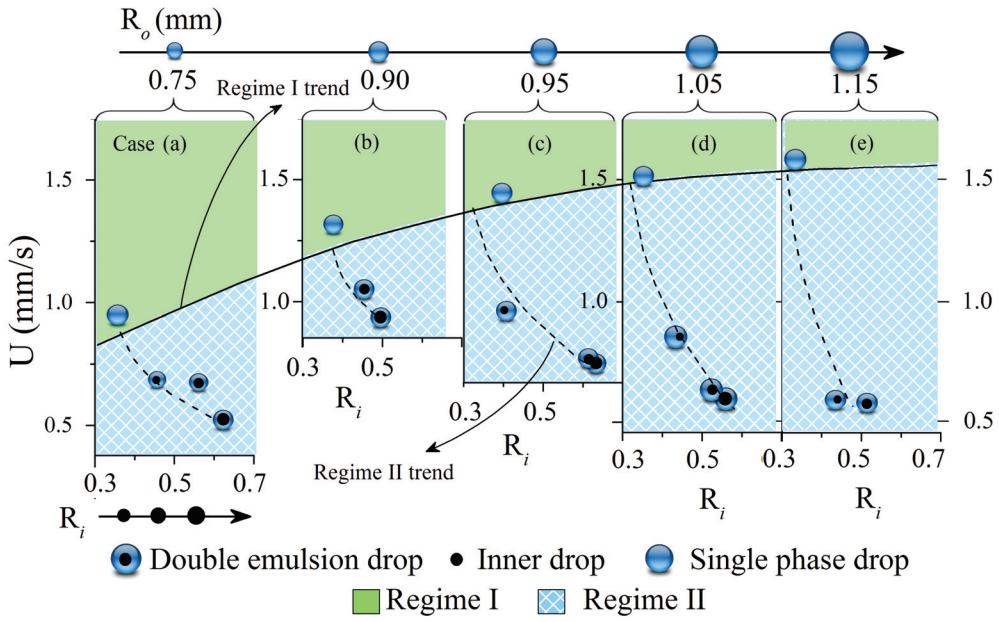

Figure 3.4: Occurrence of both regimes for drop descent with double-emulsion drop on a 3° incline. The increment in velocity with increase in size (regime I of Fig. 3.2(b)) is obtained by increasing the overall size of the drop. Increment in the droplet size is presented on the top x-axis. As presented in the hatched areas of Cases (a)-(e), Regime II behavior (decrements in the velocity) is observed with an increment in the dissipation by inserting an inner drop for a fixed outer drop size. Symbols are experimental results while the dashed and solid lines denote the velocity trend observed from the experimental data.

We introduced denser inner droplets of varied radii into the outer drops in such a way that the overall drop radius remained constant. We have termed the set of experiments with one fixed drop radius as one 'case' in Fig. 3.4. Thus cases (a) - (e) in Fig. 3.4 denote five different sets of experiments where the inner drop size is altered, maintaining a fixed overall double drop size for each particular case. For a fixed double drop size, introducing a denser inner drop increases κR of the droplet without altering the shape and the overall drop size. Thus the Stokes outer bulk dissipation remains the same for each case but the increment of κR causes

further dissipation. For a constant overall drop size, the dominant dissipation, at the contact area, results in the decrease in velocity with the increase in κR as commonly observed. The dashed lines connecting the experimental data in Fig. 3.4 highlight the Regime II, while the solid line shows the increasing trend (Regime I) of the data points. It is worth considering the role of the newly introduced interface between the outer and inner drop. Relative motion between the inner and outer drop along this interface might invite an additional internal dissipation in addition to the dissipation that occurs in the vicinity of the contact area. As discussed earlier, the viscous dissipation near the contact area scales as the fourth exponent of the characteristic radius; similarly, the additional viscous dissipation due to the relative motion at the new interface, may also scale with the same exponent of the characteristic length scale such that it may scale as $\sim Ri^4$. It is plausible that this dissipation also accounts for the decrements in velocity as the area of the interface is increased with increasing inner drop radius. The rational for scaling argument for this dissipation is from the understanding of viscous dissipation near the contact area of drop. Exact quantification of this dissipation requires further investigations in detail.

3.4 Conclusion

A liquid droplet rolling down an incline in a viscous medium attains higher velocities as its size increases upto a critical length scale. Above this length scale, velocity decreases with increasing drop size. Thus two distinct behaviors of drop rolling motion can be identified in the presence of an outer viscous medium. Viscosities of drop and medium significantly dictate the critical length restriction and the boundary between these two regimes. By altering the viscous dissipation at

the contact area without sacrificing the size restriction, non-intuitive decrements in drop velocity can be witnessed.

Chapter 4

Evaporation of Double Emulsion Droplets [1]

4.1 Introduction

The first publication on double emulsion drop [15] dates almost a century back. Despite, it's true potential in encapsulation and delivery of active materials is realized only with recent advancement in fabrication of micro-nano scale devices [6–11]. Number of important aspects of such double emulsion droplets are yet to be explored and interestingly the study of evaporation which is crucial for range of applications − from DNA mapping [12] to chip manufacturing [13] − has not been extended for multi-phase droplets, though that of a single phase droplet has been well characterized [85–90]. The importance of drop evaporation can be identified in inkjet printing and coating technologies [79, 80], self cleaning [81], biosensing [82] and droplet based micro-fluidics [83, 84]. For the phenomenon being highly sensitive to surface morphology and its chemical composition [123], it sparked numerous researchers across disciplines to conduct theoretical and experimental investigations on evaporation of single phase liquid droplets [85–90]. We

[1] A version of this chapter has been submitted for publication in Soft Matter as: Muhammad Rizwanur Rahman and Prashant R. Waghmare, "Evaporation of double emulsion drop and resurfacing of daughter droplet", 2018. Received first revision on January 22, 2018.

extended the investigation of drop evaporation to double emulsion droplets. The experimental evidences along with the modified theoretical exercise demanded to explore an anomalous observation during such evaporation process. We have observed two different but quite unique phenomena; the first one is at the end of the evaporation of the outer drop where a sudden change in the contact angle of the inner drop was noticed; the second one is the appearance of a daughter droplet after the completion of noticeable evaporation of the inner drop. These two new observations are coined along with the conventionally reported three modes of evaporation. The regime where the sudden change in contact angle occurs is termed as 'transition regime' while the unexpected occurrence of a daughter drop is referred as 'resurfacing'. Based on the phenomenological evidence of resurfacing of a daughter drop in double-emulsion drop evaporation, an hypothesis is proposed which is validated with single phase drop evaporation where the occurrence of daughter drop is also observed.

4.2 Experimental methods

Oleo-phobic substrates ($10\ cm \times 4\ cm$) were cleaned in de-ionized water and ethanol prior to each experiment. A droplet was carefully deposited and allowed to attain equilibrium configuration. The change in contact angles and three phase contact line (TPCL), represented by base diameter were recorded at 60 frames per second from side as well as top of the drop. Base diameter from the side view of the droplet was considered for further analyses. An appropriate selection of liquid combination necessitates the deposition of the inner drop from needle at the outer drop-air interface. The selection and validity of a considered model prompted us

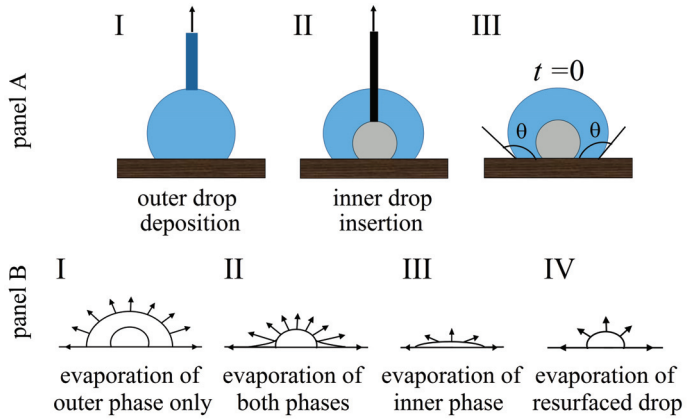

Figure 4.1: Evaporation of double emulsion drop (images are not drawn to the scale): Panel A: (I) an outer drop was deposited on a substrate followed by (II) the insertion of an inner drop carefully maintaining the concentricity of the two drops (III) evaporation of double emulsion drop is analyzed after the successful deposition of inner drop, Panel B: Different steps involved in double emulsion drop evaporation and details of (I) - (IV) is discussed in the 'Double emulsion drop evaporation' section.

to study the evaporation of single phase drop of water ($c_s = 0.017\ kg/m^3, D = 2.4 \times 10^{-5}\ m^2 s^{-1}$), diiodomethane ($c_s = 0.018\ kg/m^3, D = 6 \times 10^{-6}\ m^2 s^{-1}$) and toluene ($c_s = 0.14\ kg/m^3, D = 8 \times 10^{-6}\ m^2 s^{-1}$). For experimenting with double emulsion drop, first an outer water drop was deposited and then an inner drop of diiodomethane was inserted as illustrated in panel A of Fig. 4.1. The volume of the droplets used for the experiments varied between $0.25\ \mu L$ to $10\ \mu L$ with an instrumentation error of $\pm\ 0.01\ \mu L$. Pristine adhesive surface and acrylic sheets were used to obtain a consistent repetitive resurfacing of daughter droplet observations. Each experiments were conducted for at least 3 times and the mean of the three measurements are reported.

Table 4.1: Contact angles of different drop liquids on the substrates used for experiment

Drop liquid	Substrate	Medium	Contact Angle (°), ±3
water	oleophobic	air	80
water	adhesive	air	105
water	acrylic	air	78
water	acrylic with ring	air	85
diiodomethane	oleophobic	air	70
diiodomethane	oleophobic	water	120
diiodomethane	oleophobic	water vapor (sat.)	65
toluene	oleophobic	air	38

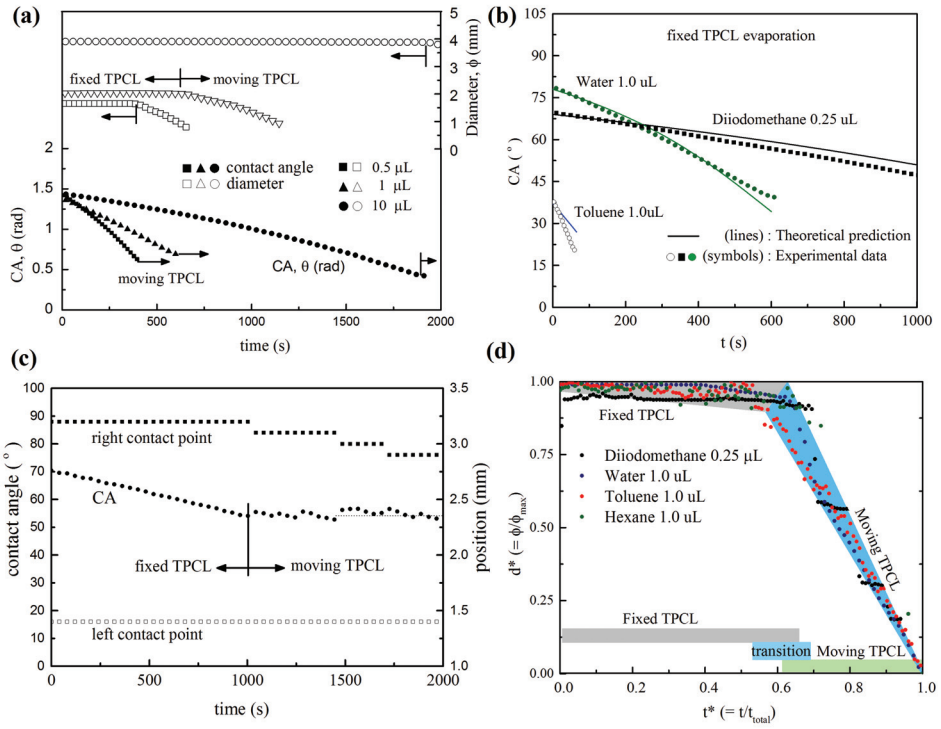

Figure 4.2: Evaporation of single phase droplets on oleophobic surface. (a) water droplets demonstrating both fixed and moving TPCL during the drying time (b) comparison between experimental data and theoretical model [124] for fixed TPCL mode of the evaporation (c) evaporation of a diiodomethane droplet − fixed TPCL mode for the first half of the drying time is followed by intermittent moving TPCL mode with a number of stick-slips (d) droplets of liquids with varying volatility follows fixed TPCL mode more than half of its drying period and the onset of transition between two modes of evaporation occurs approximately at same time fraction.

4.3 Results and Discussion

4.3.1 Single phase drop evaporation

The adaptability of the well advanced single phase droplet evaporation theory was studied by implementing the modification in the already existed models[124]. Picknett and Bexon [125], in their pioneering work, distinguished between the existence of two modes of sessile drop evaporation, namely, constant contact radius (CCR) or fixed TPCL and constant contact angle (CCA) or moving TPCL. The chaotic existence of both modes is often observed, particularly at the end of the droplet evaporation until a visual observation permits to measure the contact angle. The measurable end of the evaporation is always identified by reporting the diminishing contact angle which is quite difficult to measure below 5°. In reality the existence of the liquid thin film with finite volume is always ignored. The transition [126–130] from fixed to moving contact line occurs when the evaporating flux at the TPCL dominates over the evaporation through the liquid-vapor interface. With attainment of a critical contact angle, droplet perimeter can no longer remain pinned on the substrate and starts slipping. Thus, the moving TPCL evaporation mode is observed. This occurs, as a consequence of the competition between an intrinsic adhesion force preventing contact line motion and an exertion of a force due to evaporation flux that tends to contract the droplet [126]. For evaporation of an isolated liquid sphere in an infinite medium, rate of mass transfer follows a linear relationship with radius R as described in Maxwell's equation where the diffusive flux is used as an analogy to the electrostatic potential [131].

$$\frac{dM}{dt} = -4\pi D R \Delta c \tag{4.1}$$

Here, D is diffusion coefficient and Δc is the concentration gradient. For evaporation of a sessile droplet, contact line dynamics and surface morphology complicate the scenario where contact angle as well as base diameter of the TPCL [132, 125]dictate the dynamics. The diffusion model proposed by Popov [133] for a sessile droplet with contact radius R_c, contact angle θ takes the form of equation 4.2 :

$$\frac{dM}{dt} = \rho\frac{dV}{dt} = -\pi RD\Delta c f(\theta) \tag{4.2}$$

Here, the function $f(\theta)$ is given by the following expression

$$f(\theta) = \frac{sin\theta}{1+cos\theta} + \int_o^\infty \frac{1+cosh(2\theta\tau)}{sinh(2\pi\tau)} tanh[(\pi-\theta)\tau]d\tau \tag{4.3}$$

where τ is non-dimensional drying time. As in Fig. 4.2 (a), water droplets of different initial volumes are seen to evaporate with fixed TPCL mode at the beginning which is followed by a moving TPCL mode with diminishing base diameter [134, 135].

For a single phase droplet evaporation, as the droplet gets pinned during fixed TPCL mode, the loss in mass translates into corresponding decrements in height and contact angle until a critical contact angle is attained. Though a droplet would like to evaporate without any additional penalty in its energy by maintaining equilibrium contact angle, the pinning of the TPCL and dominant evaporation flux across the liquid-air interface inhibits the smooth decrease in contact diameter [136]. But as a critical angle is approached, the evaporation flux at the TPCL becomes large enough to surpass the energy barrier resulting in the change of base diameter. Occasionally, in this second mode of evaporation the stick-slip [137] or stick-jump behaviour of TPCL is noticed[138]. Assuming the spherical cap assumption along

with the functional variation of contact angle (Eqn 4.3), the instantaneous change of droplet contact angle in moving TPCL with fixed contact angle mode can be derived as [124]:

$$\frac{d\theta}{dt} = -\frac{D\Delta c}{\rho R^2}(1 + cos\theta)^2 f(\theta) \tag{4.4}$$

Theoretical estimations, predicted by Eq. 4.4, are compared with experimental observations as presented in Fig. 4.2 (b) for a range of droplet volumes with varied volatility and diffusion property. This clearly suggests that the selected theoretical model (Eqn. 4.4) can predict the droplet evaporation dynamics in good agreement with experimental observations. However, one can detect higher difference between the theoretical and experimental observations for highly volatile liquid drop evaporation as noticed for toluene in Fig. 4.2 (b). A special attention is given to the complete evaporation of a diiodomethane droplet since it will be used as the inner drop for double emulsion drop evaporation study. Figure 4.2 (c) suggests that in case of diiodomethane a number of 'stick-jump' [138] scenario was observed. To pinpoint this observation, the position of two ends of the base diameter is traced as depicted in Fig. 4.2 (c). In terms of the time fraction required to complete the first mode (fixed TPCL) of evaporation, interestingly, droplets of different liquids show similar evaporation behavior. In Fig. 4.2 (d), for all liquid-solid combinations considered in this study, a fixed TPCL mode of evaporation is observed for a time period more than half of the total drying time.

Single phase drop analysis is performed to get a confidence on the selection of theoretical analysis which will be extended for the double-emulsion drop evaporation.

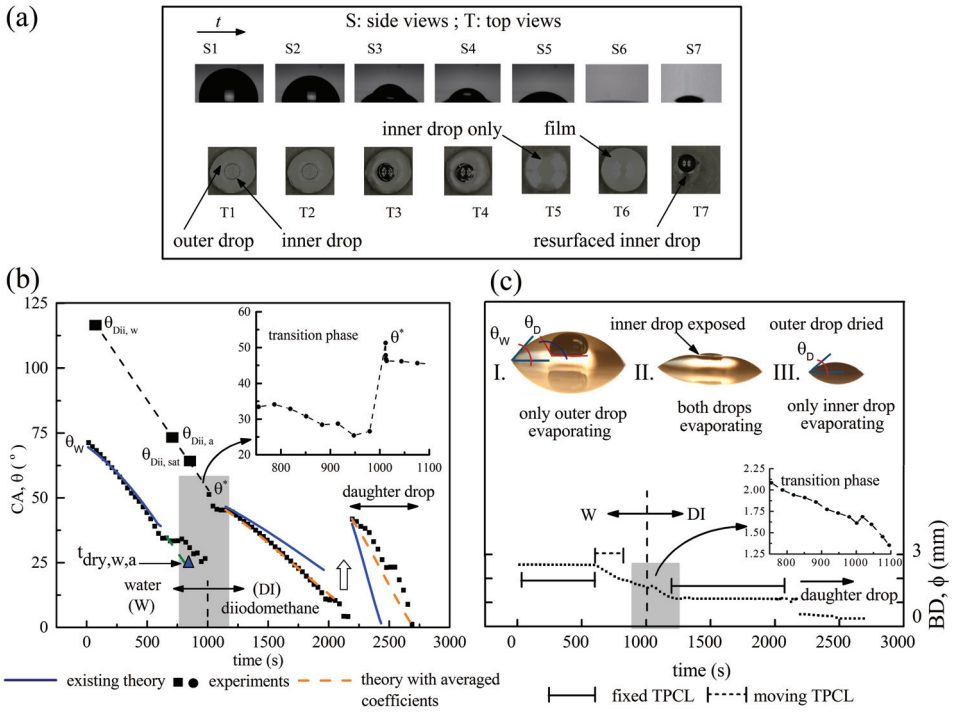

Figure 4.3: Evaporation of double emulsion drop on an oleophobic surface (a) Side and topviews of an evaporating double emulsion drop : evaporation of the outer phase followed by simultaneous evaporation of both the drop in a transition phase (S1-S4; T1-T4). Later the outer phase is completely dried and inner drop evaporates (S5;T5) until a film phase is reached (S6;T6) with nearly zero contact angle. Resurfacing of the film with appearance of a small daughter droplet (S7 ; T7). (b) Change of contact angle over time shows good qualitative agreement between observations (symbols) and theoretical prediction (continuous lines) in the outer drop evaporation region, but disagreement becomes apparent as we approach the transition regime and the inner drop evaporation. Inset shows the transition regime where the inner drop attains θ^* - that is different from the contact angle of the diiodomethane drop in air ($\theta_{DI,a}$), in water ($\theta_{DI,w}$) or in saturated water vapor ($\theta_{DI,sat}$) on the same substrate. (c) Variation of contact base diameter shows the same phenomenon with the inset depicting the transition regime. Sub-figures I, II and III are pictorial representation of three distinguished steps of the double emulsion drop evaporation.

4.3.2 Double emulsion drop evaporation

Evaporation of a double-emulsion droplet may pose a complicated scenario since there are new or modified interfaces with an additional liquid-liquid interface and

two TPCLs. A unique experimental arrangement allowed us to observe the double-emulsion drop. A diiodomethane drop is deposited inside a water drop on an oleophobic substrate. The evaporation of double emulsion drop was studied by observing the change in the contact angle and the base diameter for both the drops. Similar to a single phase drop, evaporation starts with fixed TPCL mode where the base radius remains unaltered for a considerable time period with decrease in contact angle and drop height that can be seen from Fig. 4.3(a) (Side views - S1, S2 ; Top views - T1, T2). Ensuingly, the outer phase water drop height decreases to that of the inner drop and at one point, the two interfaces interact with each other. We have termed the time period − from this interface interaction to the complete exposure of the inner droplet to air − as 'transition regime'. Since the air-water interface is shrinking due to evaporation, eventually the inner drop gets exposed to the air by forming an air-diidomethane interface. The partially exposed inner drop is shown in S3 and T3 of Fig. 4.3(a). Interestingly, during this evaporation of the outer drop, the inner drop is forced to spread on the prewetted substrate.

It is worthwhile to notice in Fig. 4.3(b) that the second mode of evaporation (moving TPCL) for outer drop was obstructed and shortened by the existence of the inner drop. The time required to complete the fixed TPCL evaporation mode for a single phase water drop is denoted as $t_{dry,w,a}$ in the figure. This is longer in comparison with the time observed in the case of the double-emulsion drop case. We speculate that one can evaporate a majority of the liquid drop with a fixed TPCL by carefully maneuvering the outer to inner drop volume or contact line radius ratios. In the considered volume ratio of water and diiodomethane drops, a very short period of a moving TPCL mode was observed. Once both the evaporating

liquids compete for the evaporation, a third mode was observed with moving TPCL with changing contact angles, where the outer drop merely existed at the bottom of the inner drop as seen in S4 and T4 (transition regime). The water drop can attain the minimum contact angle with a thin film at the inner drop base. A drastic change in the contact angle confirms the visible drying of the water, i.e., outer phase which is shown in the inset of Fig. 4.3 (b). The negligible change in the base diameter suggests the coexistence of water and diiodomethane vapor along the TPCL.

Theoretically, one can expect that the diiodomethane drop must attain equilibrium configuration ($\theta_{DI,air}$) justifying Young's equation in air medium. But it attains a new configuration (S5) which is significantly different from the equilibrium contact angle in air ($\theta_{DI,a}$) or water ($\theta_{DI,w}$) medium. The contact angles of diiodomethane in air, water medium and in saturated water vapor ($\theta_{DI,sat}$) are provided in Table 4.1 and Fig. 4.3(b). The new contact angle, (θ^*) is less than $\theta_{DI,air}$ and $\theta_{DI,sat}$ which suggests the change in the surface energy of the solid, i.e., solid-air interfacial energy. This can be attributed to the deposition of water as well as diiodomethane vapor. Ideally, the inner diiodomethane drop attains the equilibrium inside water medium with contact angle $\theta_{DI,w}$ and by the time it is exposed to air, contact angle reduces to θ^*. The transition from $\theta_{DI,w}$ to θ^* is due to the evaporation of the outer drop. We assume, this change follows similar behavior as θ_w, hence we connect $\theta_{DI,w}$ with θ^* with a dashed line parallel to the trend of θ_w and passing through $\theta_{DI,a}$ and $\theta_{DI,sat}$ as presented in Fig. 4.3 (b). As observed for saturated environment wettability studies [139], the saturated vapor reduces the contact angle. Thus we speculate that during the outer water drop evaporation the surrounding medium for the inner drop gets saturated with the water vapor which further gets

adsorbed on the solid surface. Once the outer liquid cushion is evaporated, inner drop is suddenly exposed to a different surface energy interface that results in another marginal decrease in the contact angle, $\Delta\theta \sim 5^{\circ}$ (inset of Fig. 4.3(b)) with sudden increase in base diameter, $\Delta\Phi \sim 0.1\ mm$ (inset of Fig. 4.3(c)) of the inner drop.

Quiet interestingly, for complete inner drop evaporation the fixed TPCL mode is observed as shown in the Fig. 4.3 until a sudden appearance of a daughter droplet. Hence the apparent completion of evaporation was deceiving due to the limitations of the imaging systems which generally allows to measure contact angles as low as $2 - 5^{\circ}$. We further quantified the evaporation of this resurfaced new drop which is marked as daughter droplet evaporation regime in fig. 4.3 (b) and (c). This emergence of daughter drop from an invisible (as viewed from the side) thin film motivated us to analyze the evaporation from the top view as depicted in fig. 4.3 (a). It is evident that despite the contact angle measured from side view (S6) indicate complete evaporation, the top view shows the presence of a thin-film (T6). After a few seconds, a daughter drop appears for which the contact angle and base diameter can be measured until it dries out. We have confirmed this observation multiple times and one can assure that in case of the water-diidomethane double-emulsion drop evaporation, the diiodomethane drop gets pinned during evaporation. The pinning of the contact line might be a consequence of the presence of the water vapor along the TPCL that does not allow the drop to change the mode of evaporation from fixed TPCL to moving TPCL as expected for a single drop evaporation. The resurfacing of diiodomethane drop, which is not observed in its single phase experiments, is quite interesting and emphasizes on the sensitivity towards pining of the

TPCL. To observe the resurfacing of the daughter droplet, a new set of experiments is proposed where the TPCL is forcefully pinned until the end of the evaporation and this proposed hypothesis is validated in the next section.

It is worthwhile to comment on the the theoretical modeling of evaporation, validated in Fig. 4.2 (b), for double-emulsion droplet evaporation, in particular, for inner and resurfaced daughter drop. The change in the contact angle over drying time of double-emulsion is shown in Fig. 4.3 (b) where symbols represent experimental observations and the continuous lines are predictions obtained from Eq. 4.4. It is evident that, double-emulsion drop evaporation follows the same modeling as of single phase until the onset of the transition regime. Hence, one can argue that the role of the inner drop is negligible until it starts evaporating. If we consider a single phase water drop (without inner drop) of the total volume of double emulsion drop, the fixed TPCL evaporation in air can be observed up to $t_{dry,w,a}$ as shown in the Fig.4.3 (b). But the presence of the inner drop alters the total evaporation time for outer drop as explained earlier. Since the evaporation of inner and daughter drop is mainly of fixed TPCL, it is worthwhile to extend the similar modeling approach to predict these observations. As presented for outer drop evaporation, the continuous lines represent the theoretical predictions of Eq. 4.4 for inner and daughter drop as well. It is evident that this modeling over or under predicts for inner and daughter drops. We carefully performed the parametric analysis and concluded that the presented modeling is sensitive to the concentration and diffusion of the phases involved in the evaporation. For double-emulsion drop evaporation, it is debatable whether outer or inner drop properties play a role or combined properties need to be considered. The tuning of the theoretical model suggests that while considering the

model for inner drop and daughter drop evaporation, volume weighted averaging of the concentration gradient and the diffusion coefficients is needed to be considered to predict comparable results with experimental observations. The dashed lines in Fig. 4.3 (b) depict the modified theoretical predictions with appropriate averaged properties of liquids. This modification in the diffusion and concentration is attributed to the evaporation of outer phase, i.e., presence of vapor phase of the outer liquid in the vicinity of the TPCL and the liquid-air interface. This might have altered the properties dominating the phenomenon; hence using only single phase properties (continuous lines - blue) over or under predict the experimental observations. This signifies the role of altered surrounding conditions due to the evaporation of two different liquids. Proper quantification of this alteration and the physical explanation may interest researchers for a detail study.

4.3.3 Resurfacing of daughter droplet

The observation of thin film resulting in resurfacing or appearance of the daughter droplet motivated us to investigate further into this phenomenon. It is worthwhile to investigate why such a resurfacing was never observed in the case of single phase droplet evaporation. Therefore, experiments with evaporating water droplet on a number of substrates including acrylic, copper, aluminum sheets, micro textured and adhesive surfaces were performed. Surprisingly, only adhesive coated surfaces demonstrated the resurfacing of water drops as can be seen in Fig. 4.4 (a). The top two panels depict the top and side views of the evaporating drops. Change in contact angle with corresponding base diameter is shown with filled and empty symbols, respectively.

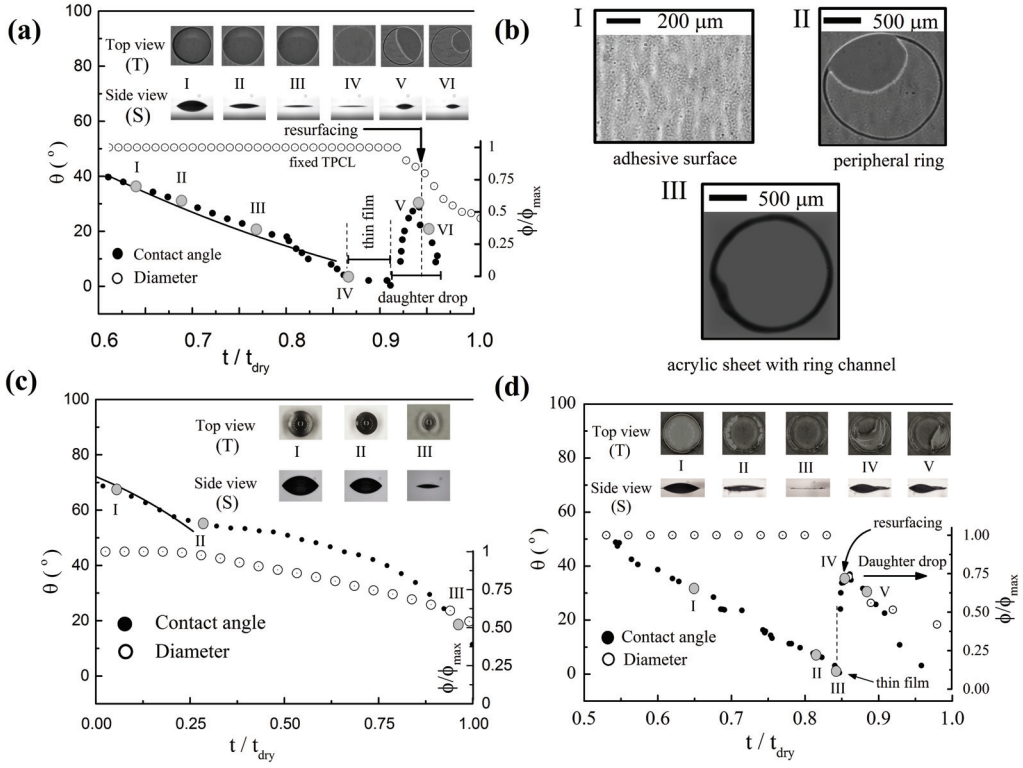

Figure 4.4: Evaporation and resurfacing of droplet. (a) evaporation on adhesive surface incorporates thin film phase and resurfacing into a smaller droplet. Top and side views corresponds to the points that are differentiated with grey circles and numbered sequentially. Experimental data for contact angles and base diameter (non dimensional) are presented with filled and empty symbols. (b) I − microscopic view of the adhesive surface shows the micro-nano features of the surface (b) II − a ring like impression creates local pinning sites along the TPCL (b) III − a micro metric ring is machined on an acrylic sheet to dummy the ring effect (c) water drop evaporation on a acrylic sheet without ring shows no film phase or resurfacing (d) with the ring on the acrylic sheet distinct thin film phase followed by resurfacing of a daughter droplet is seen.

The dominance of fixed TPCL evaporation mode convinced us to conclude that if fixed TPCL evaporation can be significantly prolonged over the drying time, one can observe the resurfacing of the daughter droplet. Fig. 4.4 (a) mainly focuses on the end of the fixed TPCL evaporation until it reaches the smallest measurable contact angle. Different stages presented in the panel are denoted along the change in the contact angle with roman numbers. Careful microscopic observation of the adhesives layer suggests that the surface contains micro-nano features (Fig. 4.4 (b) - I). Thus the surface facilitates the pinning of the contact line which eventually forces the drop to form a film before the daughter drop formation. In this case, while the daughter drop resurfaces, a big jump in contact angle (from 0 to 30°) is noticed as shown in Fig. 4.4 (a).

To view the film and resurfacing of the drop, the camera viewing angle was slightly tilted $(\sim 2^{\circ})$ which demonstrates thin film in side views (III and IV) as well as corresponding top views. The pinning of the TPCL can be confirmed by ring like impression similar to 'coffee stain ring' as shown in Fig. 4.4 (b) - II. This ring acts as a peripheral pinning location that holds the droplet until it converges to a thin film with vanishing contact angle. However, it is well established that, if the evaporating flux at TPCL is significantly larger than the evaporation flux across the liquid-air interface, it surpasses the pinning strength and hence, moving TPCL evaporation can be observed. In case of the evaporation on adhesive surface, we speculate that the evaporation flux is not large enough until the drop attains the thin film. The moment the evaporation across the air-liquid interface of thin film is not dominant enough, resurfacing triggers into the formation of daughter drop as shown in Fig. 4.4 (a) IV $-$ VI. However, a double emulsion or a single diiodomethane

drop do not exhibit such behavior on this particular substrate emphasizing on the dependency or sensitivity of this phenomenon on surface-liquid combinations.

With the observation of resurfacing, we identified a critical aspect that dictates the formation of the daughter droplet, i.e., pinning of the contact line for entire evaporation of the droplet. To validate this proposed hypothesis, we artificially created a physical barrier by engraving a ring on an acrylic substrate. This artificial ring of $1.5mm$ diameter is of the same dimension as that of the base diameter of water drop of a given volume as shown in Fig. 4.4 (b) -III. For comparison, we initially studied the water drop evaporation on an acrylic substrate without any ring as shown in Fig. 4.4(c) which clearly demonstrates the usual modes of the evaporation. Top and side views at three different time instants also depicts the movement of the TPCL. Since there is no pinning of the three phase contact line, we cannot expect a thin film phase and subsequent resurfacing.

Discordantly, when evaporation of water drop is observed on the same substrate with a ring (with micro metric depth of $\sim 100\mu m$), we observe the prolongation of fixed TPCL mode over almost the entire drying period as shown in Fig. 4.4 (d). The drop remains pinned along the TPCL (S I, S II ; T I, T II) until the contact angle reaches zero and forms a thin film (T III; S III). This is followed by the resurfacing of a daughter droplet (S IV, S V ; T IV, T V) as hypothesized, with a jump in contact angle as depicted in the plot along with associated decrease in base diameter. Thus, by employing our hypothesis *i.e.,* forcefully pinning the TPCL, resurfacing of a daughter droplet is demonstrated on a regular substrate which otherwise doesn't behave similarly.

4.4 Conclusion

Evaporation of a double emulsion drop has been investigated in detail. The evaporation of corresponding single phase drops well agree with existing theoretical model, however significant deviations have been observed for the double drop case. A modified theoretical approach agrees with the observed evaporation modes for the double emulsion drops. Evaporation of such droplet exhibits the commonly observed modes of evaporation with two new regimes in its drying time that are identified in this study. The transition regime from outer to inner drop constitutes a sudden spreading of the inner droplet which results in a wetting scenario that is different from the theoretically expected equilibrium configuration for similar liquid-solid-vapor combination. The sudden change in the contact angle imprints the complete drying of the outer drop liquid and can be attributed to complete exposure of the inner droplet to environment. A resurfacing of a daughter droplet is witnessed after the commonly identified completion of the evaporation. This observation is critically investigated and attributed to the pinning of the three phase contact line. Later, we forcefully pinned the three phase contact line of a single phase droplet by carefully engineering a substrate and a mechanism of daughter droplet resurfacing from thin film is established.

Chapter 5

Conclusion

5.1 Summary

This thesis addresses three fundamental aspects of multiphase microfluids where surface and interfacial factors dictate the outcome. Our particular attention revolves around rolling, evaporation and spreading of compound micro drops; however, the single phase analogues are also critically investigated for the establishment of the demarcation.

The first fundamental aspect studied here is spreading and Chapter 2 discusses the early time drop spreading on a liquid-fluid interface. Unlike spreading on solid substrate, a drop deforms at three phase contact line (TPCL) as it spreads on a liquid-fluid interface. Present observations strongly suggest the short time dynamics to be independent of the interface property. Quite interestingly, spreading shows a logarithmic response rather than the classical power law. Experimental observations allowed us to establish a simple empirical expression to predict the temporal growth of the contact radius. Further, inertial oscillation are observed for spreading of less viscous drop that has been described in similar way as of inertial capillarity. Understanding the interfacial dynamics and the associated time scale enables

successful generation of compound drop system which broadens our exploration spectrum. Thus a natural extension of our investigation involves the under liquid rolling dynamics and evaporation of double emulsion droplets.

In Chapter 3, rolling dynamics is studied in detail, where scaling analysis with experimental evidences demonstrate that in creeping flow, medium viscosity significantly alters the descent speed of a drop and its dependency on drop size. In a viscous medium, while a descending drop that rolls on an incline, may travel with either increasing or decreasing velocities as its size increases. This has never been established before with a unified theory and experiments. Theoretical understandings of the role of medium viscosity allow us to establish the criteria to define these two contrasting behaviors. The transition from one to the other behavior strongly depends on the drop and medium viscosity. For a single phase drop, it is practically very difficult, if not impossible, to engineer such a drop that can demonstrate both the increasing and decreasing behaviors. The double emulsion drop provided a feasible solution due to its compound nature. Understanding the dynamics of such multiphase droplets allows superior control over the transformation from one to the other velocity behavior.

The final aspect studied here is the evaporation of such a multi-component droplet. Chapter 4 describes this study that identifies two new modes of the evaporation, namely, 'transition' and 'resurfacing'. The 'transition regime' constitutes a sudden spreading of the inner droplet as an indicator of the complete drying of outer phase drop. After the apparently complete drying of the inner drop, surprisingly, a daughter droplet resurfaces. We propose a hypothesis toward this phenomenon which allows us to reproduce the resurfacing in case of a single phase droplet.

In summary, the contribution of this thesis to the existing literature is as follows:

- Recognizing logarithmic response of spreading radius as opposed to the classical power law response
- Identification of a regime where the popularly discussed ‘counter-intuitive velocity behavior’ doesn’t apply for drop rolling on an incline, rather an intuitive behavior emanates
- Confirmation of the co-existence of contradicting velocity behaviors by means of a compound drop system, which is otherwise impossible to demonstrate experimentally
- Pinpointing two new modes of evaporation for double emulsion droplets
- Establishment of a control mechanism to prolong fixed three phase contact line evaporation and thereby facilitate resurfacing of a daughter drop from a disappearing thin film

5.2 Scope of Future Work

The findings from this thesis highlight some challenges as well as opportunities. In particular, this study progresses from simple to compound droplet systems and to deformable liquid-fluid interfaces instead of usual rigid interface studies. The identification of a logarithmic response in case of drop spreading on liquid-fluid interface and the coalescence like behavior of spreading may motivate researchers in pinpointing the link between these two seemingly different phenomena. An important step forward would be to investigate whether the spreading of a single drop on a liquid-fluid interface can emulate the coalescence of two droplets. The temporal growth of spreading diameter may correspond to the coalescing bridge growth under appropriate considerations of the associated parameters. Further, the study of multi-phase droplet spreading is expected to showcase different interface behavior and configurations. Specially, studying the spreading in case of electro or magneto wetting will be interesting topics to add value in the scientific community.

An extension to the compound drop rolling study can be the investigation of encapsulated bubble motion. If the encapsulated bubble size is increased, the increased buoyant force should result in reduced contact area and hence reduced viscous dissipation. So, in light with the presented scaling arguments for rolling drops, velocity should increase with increasing bubble size for same outer drop dimension. Thus another control mechanism of the descending speed can be established.

The study of double emulsion droplet evaporation can also be extended to the study on the effect of drop volatility. It may interest the researchers to find how volatility of drops plays a role in the compound drop evaporation. The events of

contact line stretching and daughter drop formation observed in this present study might get altered in such cases. Complete understanding of the alteration of pinning effect and prolongation of fixed contact line evaporation may lead to the exact quantification of the parameters resulting in the resurfacing phenomenon. This will, in turn, allow us to manipulate the pinning effect and the duration of evaporation modes, and thereby, complete dominance over the evaporation modes may be possible to achieve.

Bibliography

[1] V. Misuk, A. Mai, K. Giannopoulos, F. Alobaid, B. Epple, and H. Loewe, "Micro magnetofluidics: droplet manipulation of double emulsions based on paramagnetic ionic liquids," *Lab on a Chip*, vol. 13, no. 23, pp. 4542–4548, 2013.

[2] A. Sciambi and A. R. Abate, "Adding reagent to droplets with controlled rupture of encapsulated double emulsions," *Biomicrofluidics*, vol. 7, no. 4, p. 044112, 2013.

[3] E. Dolgin, "Encapsulate this," 2014.

[4] X. Zhao, J. Kim, C. A. Cezar, N. Huebsch, K. Lee, K. Bouhadir, and D. J. Mooney, "Active scaffolds for on-demand drug and cell delivery," *Proceedings of the National Academy of Sciences*, vol. 108, no. 1, pp. 67–72, 2011.

[5] J. Charve and G. A. Reineccius, "Encapsulation performance of proteins and traditional materials for spray dried flavors," *Journal of agricultural and food chemistry*, vol. 57, no. 6, pp. 2486–2492, 2009.

[6] S.-H. Kim, J. W. Kim, J.-C. Cho, and D. A. Weitz, "Double-emulsion drops with ultra-thin shells for capsule templates," *Lab on a Chip*, vol. 11, no. 18, pp. 3162–3166, 2011.

[7] H. Song, J. D. Tice, and R. F. Ismagilov, "A microfluidic system for controlling reaction networks in time," *Angewandte Chemie International Edition*, vol. 115, no. 7, pp. 792–796, 2003.

[8] S. Okushima, T. Nisisako, T. Torii, and T. Higuchi, "Controlled production of monodisperse double emulsions by two-step droplet breakup in microfluidic devices," *Langmuir*, vol. 20, no. 23, pp. 9905–9908, 2004.

[9] C. B. Chang, J. N. Wilking, S.-H. Kim, H. C. Shum, and D. A. Weitz, "Monodisperse emulsion drop microenvironments for bacterial biofilm growth," *Small*, vol. 11, no. 32, pp. 3954–3961, 2015.

[10] P.-W. Ren, X.-J. Ju, R. Xie, and L.-Y. Chu, "Monodisperse alginate microcapsules with oil core generated from a microfluidic device," *Journal of Colloid and Interface Science*, vol. 343, no. 1, pp. 392–395, 2010.

[11] H. Zhang, E. Tumarkin, R. Peerani, Z. Nie, R. M. A. Sullan, G. C. Walker, and E. Kumacheva, "Microfluidic production of biopolymer microcapsules with controlled morphology," *Journal of the American Chemical Society*, vol. 128, no. 37, pp. 12 205–12 210, 2006.

[12] A. Wu, L. Yu, Z. Li, H. Yang, and E. Wang, "Atomic force microscope investigation of large-circle dna molecules," *Analytical Biochemistry*, vol. 325, no. 2, pp. 293–300, 2004.

[13] V. Dugas, J. Broutin, and E. Souteyrand, "Droplet evaporation study applied to dna chip manufacturing," *Langmuir*, vol. 21, no. 20, pp. 9130–9136, 2005.

[14] M. Iqbal, N. Zafar, H. Fessi, and A. Elaissari, "Double emulsion solvent evaporation techniques used for drug encapsulation," *International journal of pharmaceutics*, vol. 496, no. 2, pp. 173–190, 2015.

[15] W. Seifriz, "Studies in emulsions," *Journal of Physical Chemistry A*, vol. 29, pp. 738–749, 1925.

[16] S. Sadhal and H. Oguz, "Stokes flow past compound multiphase drops: the case of completely engulfed drops/bubbles," *Journal of Fluid Mechanics*, vol. 160, pp. 511–529, 1985.

[17] S. Matsumoto, T. Inoue, M. Kohda, and K. Ikura, "Water permeability of oil layers in w/o/w emulsions under osmotic pressure gradients," *Journal of Colloid and Interface Science*, vol. 77, no. 2, pp. 555–563, 1980.

[18] A. Florence and D. Whitehill, "The formulation and stability of multiple emulsions," *International Journal of Pharmaceutics*, vol. 11, no. 4, pp. 277–308, 1982.

[19] G. Muschiolik and E. Dickinson, "Double emulsions relevant to food systems: preparation, stability, and applications," *Comprehensive Reviews in Food Science and Food Safety*, vol. 16, no. 3, pp. 532–555, 2017.

[20] H. Stone and L. Leal, "Breakup of concentric double emulsion droplets in linear flows," *Journal of Fluid Mechanics*, vol. 211, pp. 123–156, 1990.

[21] A. G. Gaonkar, "Stable multiple emulsions comprising interfacial gelatinous layer, flavor-encapsulating multiple emulsions and low/no-fat food products comprising the same," Jul. 26 1994, uS Patent 5,332,595.

[22] C. Lobato-Calleros, E. Rodriguez, O. Sandoval-Castilla, E. Vernon-Carter, and J. Alvarez-Ramirez, "Reduced-fat white fresh cheese-like products obtained from w 1/o/w 2 multiple emulsions: Viscoelastic and high-resolution image analyses," *Food Research International*, vol. 39, no. 6, pp. 678–685, 2006.

[23] S. P. Dwyer, D. OBeirne, D. Ní Eidhin, and B. T. OKennedy, "Effects of green tea extract and α-tocopherol on the lipid oxidation rate of omega-3 oils, incorporated into table spreads, prepared using multiple emulsion technology," *Journal of food science*, vol. 77, no. 12, 2012.

[24] P. Eslami, L. Davarpanah, and F. Vahabzadeh, "Encapsulating role of β-cyclodextrin in formation of pickering water-in-oil-in-water (w 1/o/w 2) double emulsions containing lactobacillus dellbrueckii," *Food Hydrocolloids*, vol. 64, pp. 133–148, 2017.

[25] A. Oppermann, B. Piqueras-Fiszman, C. De Graaf, E. Scholten, and M. Stieger, "Descriptive sensory profiling of double emulsions with gelled and non-gelled inner water phase," *Food Research International*, vol. 85, pp. 215–223, 2016.

[26] H. C. Shum, A. Bandyopadhyay, S. Bose, and D. A. Weitz, "Double emulsion droplets as microreactors for synthesis of mesoporous hydroxyapatite," *Chemistry of Materials*, vol. 21, no. 22, pp. 5548–5555, 2009.

[27] J. J. Agresti, E. Antipov, A. R. Abate, K. Ahn, A. C. Rowat, J.-C. Baret, M. Marquez, A. M. Klibanov, A. D. Griffiths, and D. A. Weitz, "Ultrahigh-

throughput screening in drop-based microfluidics for directed evolution," *Proceedings of the National Academy of Sciences*, vol. 107, no. 9, pp. 4004–4009, 2010.

[28] I. Brigger, C. Dubernet, and P. Couvreur, "Nanoparticles in cancer therapy and diagnosis," *Advanced drug delivery reviews*, vol. 54, no. 5, pp. 631–651, 2002.

[29] S. Nakhare and S. Vyas, "Preparation and characterization of multiple emulsion based systems for controlled diclofenac sodium release," *Journal of microencapsulation*, vol. 13, no. 3, pp. 281–292, 1996.

[30] W. Wang, T. Jones, and D. Harding, "On-chip double emulsion droplet assembly using electrowetting-on-dielectric and dielectrophoresis," *Fusion Science and Technology*, vol. 59, no. 1, pp. 240–249, 2011.

[31] Z.-M. Bei, T. Jones, and A. Tucker-Schwartz, "Forming concentric double-emulsion droplets using electric fields," *Journal of Electrostatics*, vol. 67, no. 2, pp. 173–177, 2009.

[32] R. Bernewitz, U. Schmidt, H. Schuchmann, and G. Guthausen, "Structure of and diffusion in o/w/o double emulsions by clsm and nmr–comparison with w/o/w," *Colloids and Surfaces A: Physicochemical and Engineering Aspects*, vol. 458, pp. 10–18, 2014.

[33] I. Scherze, K. Marzilger, and G. Muschiolik, "Emulsification using micro porous glass (mpg): surface behaviour of milk proteins," *Colloids and Surfaces B: Biointerfaces*, vol. 12, no. 3, pp. 213–221, 1999.

[34] R. Jiménez-Alvarado, C. Beristain, L. Medina-Torres, A. Román-Guerrero, and E. Vernon-Carter, "Ferrous bisglycinate content and release in w 1/o/w 2 multiple emulsions stabilized by protein–polysaccharide complexes," *Food Hydrocolloids*, vol. 23, no. 8, pp. 2425–2433, 2009.

[35] B. Li, Y. Jiang, F. Liu, Z. Chai, Y. Li, and X. Leng, "Study of the encapsulation efficiency and controlled release property of whey protein isolate–polysaccharide complexes in w1/o/w2 double emulsions," *International journal of food engineering*, vol. 7, no. 3, 2011.

[36] S. Y. Tang and M. Sivakumar, "Design and evaluation of aspirin-loaded water-in-oil-in-water submicron multiple emulsions generated using two-stage ultrasonic cavitational emulsification technique," *Asia-Pacific Journal of Chemical Engineering*, vol. 7, no. S1, 2012.

[37] N. Aditya, S. Aditya, H. Yang, H. W. Kim, S. O. Park, and S. Ko, "Co-delivery of hydrophobic curcumin and hydrophilic catechin by a water-in-oil-in-water double emulsion," *Food chemistry*, vol. 173, pp. 7–13, 2015.

[38] I. Scherze, R. Knöfel, and G. Muschiolik, "Automated image analysis as a control tool for multiple emulsions," *Food Hydrocolloids*, vol. 19, no. 3, pp. 617–624, 2005.

[39] N. Khalid, I. Kobayashi, M. A. Neves, K. Uemura, M. Nakajima, and H. Nabetani, "Monodisperse w/o/w emulsions encapsulating l-ascorbic acid: Insights on their formulation using microchannel emulsification and stability

studies," *Colloids and Surfaces A: Physicochemical and Engineering Aspects*, vol. 458, pp. 69–77, 2014.

[40] K. Schroën, O. Bliznyuk, K. Muijlwijk, S. Sahin, and C. C. Berton-Carabin, "Microfluidic emulsification devices: from micrometer insights to large-scale food emulsion production," *Current Opinion in Food Science*, vol. 3, pp. 33–40, 2015.

[41] M. Akhtar and E. Dickinson, "Water-in-oil-in-water multiple emulsions stabilized by polymeric and natural emulsifiers," *Food Colloids: fundamentals of formulation. Cambrige: The Royal Society of Chemistry*, pp. 133–143, 2001.

[42] I. Burgaud, E. Dickinson, and P. Nelson, "An improved high-pressure homogenizer for making fine emulsions on a small scale," *International journal of food science & technology*, vol. 25, no. 1, pp. 39–46, 1990.

[43] Y. Hemar, L. J. Cheng, C. M. Oliver, L. Sanguansri, and M. Augustin, "Encapsulation of resveratrol using water-in-oil-in-water double emulsions," *Food Biophysics*, vol. 5, no. 2, pp. 120–127, 2010.

[44] S. Cofrades, I. Antoniou, M. Solas, A. Herrero, and F. Jiménez-Colmenero, "Preparation and impact of multiple (water-in-oil-in-water) emulsions in meat systems," *Food chemistry*, vol. 141, no. 1, pp. 338–346, 2013.

[45] J. Xiang, F. Liu, R. Fan, and Y. Gao, "Physicochemical stability of citral emulsions stabilized by milk proteins (lactoferrin, α-lactalbumin, β-

lactoglobulin) and beet pectin," *Colloids and Surfaces A: Physicochemical and Engineering Aspects*, vol. 487, pp. 104–112, 2015.

[46] P. R. Waghmare, S. Das, and S. K. Mitra, "Drop deposition on under-liquid low energy surfaces," *Soft Matter*, vol. 9, no. 31, pp. 7437–7447, 2013.

[47] P. R. Waghmare, S. Mitra, N. S. K. Gunda, and S. K. Mitra, "Needle-free drop deposition: the role of elastic membranes," *RSC Advances*, vol. 5, no. 100, pp. 82 374–82 380, 2015.

[48] F. E. Neumann, *Vorlesungen über mathematische Physik: Vorlesungen über die Theorie der Capillarität*. BG Teubner, 1894, vol. 7.

[49] P.-G. De Gennes, F. Brochard-Wyart, and D. Quéré, *Capillarity and wetting phenomena: drops, bubbles, pearls, waves*. Springer Science & Business Media, 2013.

[50] T. Young, "An essay on the cohesion of fluids," *Philosophical Transactions of the Royal Society of London*, vol. 95, pp. 65–87, 1805.

[51] F. Brochard-Wyart and P. De Gennes, "Dynamics of partial wetting," *Advances in colloid and interface science*, vol. 39, pp. 1–11, 1992.

[52] L. Tanner, "The spreading of silicone oil drops on horizontal surfaces," *Journal of Physics D: Applied Physics*, vol. 12, no. 9, p. 1473, 1979.

[53] H. E. Huppert, "The propagation of two-dimensional and axisymmetric viscous gravity currents over a rigid horizontal surface," *Journal of Fluid Mechanics*, vol. 121, pp. 43–58, 1982.

[54] M. J. De Ruijter, J. De Coninck, and G. Oshanin, "Droplet spreading: partial wetting regime revisited," *Langmuir*, vol. 15, no. 6, pp. 2209–2216, 1999.

[55] P. J. Haley and M. J. Miksis, "The effect of the contact line on droplet spreading," *Journal of Fluid Mechanics*, vol. 223, pp. 57–81, 1991.

[56] L. Leger and J. Joanny, "Liquid spreading," *Reports on Progress in Physics*, vol. 55, no. 4, p. 431, 1992.

[57] Z. Cao and A. V. Dobrynin, "Polymeric droplets on soft surfaces: From neumanns triangle to youngs law," *Macromolecules*, vol. 48, no. 2, pp. 443–451, 2015.

[58] A. Marchand, S. Das, J. H. Snoeijer, and B. Andreotti, "Contact angles on a soft solid: From youngs law to neumanns law," *Physical review letters*, vol. 109, no. 23, p. 236101, 2012.

[59] J. C. Bird, S. Mandre, and H. A. Stone, "Short-time dynamics of partial wetting," *Physical review letters*, vol. 100, no. 23, p. 234501, 2008.

[60] A.-L. Biance, C. Clanet, and D. Quéré, "First steps in the spreading of a liquid droplet," *Physical Review E*, vol. 69, no. 1, p. 016301, 2004.

[61] A. Eddi, K. G. Winkels, and J. H. Snoeijer, "Short time dynamics of viscous drop spreading," *Physics of fluids*, vol. 25, no. 1, p. 013102, 2013.

[62] B. Roman and J. Bico, "Elasto-capillarity: deforming an elastic structure with a liquid droplet," *Journal of Physics: Condensed Matter*, vol. 22, no. 49, p. 493101, 2010.

[63] K. R. Shull, "Contact mechanics and the adhesion of soft solids," *Materials Science and Engineering: R: Reports*, vol. 36, no. 1, pp. 1–45, 2002.

[64] G. J. Elfring and G. Goyal, "The effect of gait on swimming in viscoelastic fluids," *Journal of Non-Newtonian Fluid Mechanics*, vol. 234, pp. 8–14, 2016.

[65] G. G. Stokes, *On the effect of the internal friction of fluids on the motion of pendulums*. Pitt Press Cambridge, 1851, vol. 9.

[66] G. Galili, "Dialogues concerning two new sciences," *New York: Macmillan*, vol. 1, p. 105, 1914.

[67] R. Woodward, *Transactions of the New York Academy of Sciences*, p. 2, 1895.

[68] H. Allen, "L. The motion of a sphere in a viscous fluid," *Philosophical Magazine Series 5*, vol. 50, no. 306, pp. 519–534, 1900.

[69] L. Rayleigh, "On the motion of solid bodies through viscous liquid," *Philosophical Magazine Series 6*, vol. 21, no. 126, pp. 697–711, 1911.

[70] P. G. Saffman, "The lift on a small sphere in a slow shear flow," *Journal of Fluid Mechanics*, vol. 22, no. 02, p. 385, 1965.

[71] A. N. Prokunin, "On a paradox in the motion of a rigid particle along a wall in a fluid," *Fluid Dynamics*, vol. 38, no. 3, pp. 443–457, 2003.

[72] R. Gohar, *Elastohydrodynamics*. World Scientific, 2001.

[73] J. Bico, J. Ashmore-Chakrabarty, G. McKinley, and H. Stone, "Rolling stones: The motion of a sphere down an inclined plane coated with a thin liquid film," *Physics of fluids*, vol. 21, no. 8, p. 082103, 2009.

[74] J. A. Schwartz, J. V. Vykoukal, and P. R. C. Gascoyne, "Droplet-based chemistry on a programmable micro-chip," *Lab on a Chip*, vol. 4, no. 1, p. 11, 2004.

[75] G. Katsikis, J. S. Cybulski, and M. Prakash, "Synchronous universal droplet logic and control," *Nature Physics*, vol. 11, no. 7, pp. 588–596, 2015.

[76] D. R. Link, E. Grasland-Mongrain, A. Duri, F. Sarrazin, Z. Cheng, G. Cristobal, M. Marquez, and D. A. Weitz, "Electric control of droplets in microfluidic devices," *Angewandte Chemie International Edition*, vol. 45, no. 16, pp. 2556–2560, 2006.

[77] L. Mahadevan and Y. Pomeau, "Rolling droplets," *Physics of fluids*, vol. 11, no. 9, pp. 2449–2453, 1999.

[78] D. Richard and D. Quéré, "Viscous drops rolling on a tilted non-wettable solid," *Europhysics Letters*, vol. 48, no. 3, p. 286, 1999.

[79] E. L. Talbot, L. Yang, A. Berson, and C. D. Bain, "Control of the particle distribution in inkjet printing through an evaporation-driven sol–gel transition," *ACS Applied Materials Interfaces*, vol. 6, no. 12, pp. 9572–9583, 2014.

[80] P. Calvert, "Inkjet printing for materials and devices," *Chemistry of Materials*, vol. 13, no. 10, pp. 3299–3305, 2001.

[81] R. Blossey, "Self-cleaning surfacesvirtual realities," *Nature Materials*, vol. 2, no. 5, pp. 301–306, 2003.

[82] F. De Angelis, F. Gentile, F. Mecarini, G. Das, M. Moretti, P. Candeloro, M. Coluccio, G. Cojoc, A. Accardo, C. Liberale *et al.*, "Breaking the diffusion limit with super-hydrophobic delivery of molecules to plasmonic nanofocusing sers structures," *Nature Photonics*, vol. 5, no. 11, pp. 682–687, 2011.

[83] S. T. Chang and O. D. Velev, "Evaporation-induced particle microseparations inside droplets floating on a chip," *Langmuir*, vol. 22, no. 4, pp. 1459–1468, 2006.

[84] Q. Li, Y. T. Zhu, I. A. Kinloch, and A. H. Windle, "Self-organization of carbon nanotubes in evaporating droplets," *Journal of Physical Chemistry B*, vol. 110, no. 28, pp. 13 926–13 930, 2006.

[85] C. N. Kaplan and L. Mahadevan, "Evaporation-driven ring and film deposition from colloidal droplets," *Journal of Fluid Mechanics*, vol. 781, 2015.

[86] X. Man and M. Doi, "Ring to mountain transition in deposition pattern of drying droplets," *Physical Review Letters*, vol. 116, no. 6, p. 066101, 2016.

[87] A.-M. Cazabat and G. Guéna, "Evaporation of macroscopic sessile droplets," *Soft Matter*, vol. 6, no. 12, pp. 2591–2612, 2010.

[88] H. Y. Erbil, G. McHale, and M. Newton, "Drop evaporation on solid surfaces: constant contact angle mode," *Langmuir*, vol. 18, no. 7, pp. 2636–2641, 2002.

[89] H. Hu and R. G. Larson, "Evaporation of a sessile droplet on a substrate," *Journal of Physical Chemistry B*, vol. 106, no. 6, pp. 1334–1344, 2002.

[90] J. M. Stauber, S. K. Wilson, B. R. Duffy, and K. Sefiane, "On the lifetimes of evaporating droplets," *Journal of Fluid Mechanics*, vol. 744, 2014.

[91] I. G. Hwang, J. Y. Kim, and B. M. Weon, "Droplet evaporation with complexity of evaporation modes," *Applied Physics Letters*, vol. 110, no. 3, p. 031602, 2017.

[92] G. Garnier, M. Bertin, and M. Smrckova, "Wetting dynamics of alkyl ketene dimer on cellulosic model surfaces," *Langmuir*, vol. 15, no. 22, pp. 7863–7869, 1999.

[93] A. Milchev and K. Binder, "Droplet spreading: A monte carlo test of tanners law," *The Journal of chemical physics*, vol. 116, no. 17, pp. 7691–7694, 2002.

[94] S. L. Cormier, J. D. McGraw, T. Salez, E. Raphaël, and K. Dalnoki-Veress, "Beyond tanners law: Crossover between spreading regimes of a viscous droplet on an identical film," *Physical review letters*, vol. 109, no. 15, p. 154501, 2012.

[95] L. Leger, M. Erman, A. Guinet-Picard, D. Ausserre, and C. Strazielle, "Precursor film profiles of spreading liquid drops," *Physical review letters*, vol. 60, no. 23, p. 2390, 1988.

[96] D. Ausserré, A. Picard, and L. Léger, "Existence and role of the precursor

film in the spreading of polymer liquids," *Physical review letters*, vol. 57, no. 21, p. 2671, 1986.

[97] Y. Gu and D. Li, "A model for a liquid drop spreading on a solid surface," *Colloids and Surfaces A: Physicochemical and Engineering Aspects*, vol. 142, no. 2, pp. 243–256, 1998.

[98] D. Bonn, J. Eggers, J. Indekeu, J. Meunier, and E. Rolley, "Wetting and spreading," *Reviews of modern physics*, vol. 81, no. 2, p. 739, 2009.

[99] C. Ma, S. Bai, X. Peng, and Y. Meng, "Transient spreading of water droplet on laser micro-structured sic surfaces," *Applied Surface Science*, vol. 311, pp. 789–792, 2014.

[100] N. Savva, S. Kalliadasis, and G. A. Pavliotis, "Two-dimensional droplet spreading over random topographical substrates," *Physical review letters*, vol. 104, no. 8, p. 084501, 2010.

[101] G. McHale, C. Brown, and N. Sampara, "Voltage-induced spreading and superspreading of liquids," *Nature communications*, vol. 4, p. 1605, 2013.

[102] A. Carlson, M. Do-Quang, and G. Amberg, "Dissipation in rapid dynamic wetting," *Journal of Fluid Mechanics*, vol. 682, pp. 213–240, 2011.

[103] J. Dervaux and L. Limat, "Contact lines on soft solids with uniform surface tension: analytical solutions and double transition for increasing deformability," in *Proc. R. Soc. A*, vol. 471, no. 2176. The Royal Society, 2015, p. 20140813.

[104] S. J. Park, B. M. Weon, J. San Lee, J. Lee, J. Kim, and J. H. Je, "Visualization of asymmetric wetting ridges on soft solids with x-ray microscopy," *Nature communications*, vol. 5, 2014.

[105] L. A. Lubbers, J. H. Weijs, L. Botto, S. Das, B. Andreotti, and J. H. Snoeijer, "Drops on soft solids: free energy and double transition of contact angles," *Journal of fluid mechanics*, vol. 747, 2014.

[106] J. Sebilleau, "Equilibrium thickness of large liquid lenses spreading over another liquid surface," *Langmuir*, vol. 29, no. 39, pp. 12 118–12 128, 2013.

[107] R. Shabani, R. Kumar, and H. J. Cho, "Droplets on liquid surfaces: Dual equilibrium states and their energy barrier," *Applied Physics Letters*, vol. 102, no. 18, p. 184101, 2013.

[108] M. R. Rahman and P. R. Waghmare, "Influence of outer medium viscosity on the motion of rolling droplets down an incline (accepted)," *Physical Review Fluids*, 2018.

[109] J. M. Kolinski, L. Mahadevan, and S. Rubinstein, "Drops can bounce from perfectly hydrophilic surfaces," *EPL (Europhysics Letters)*, vol. 108, no. 2, p. 24001, 2014.

[110] D. Quéré, É. Raphaël, and J.-Y. Ollitrault, "Rebounds in a capillary tube," *Langmuir*, vol. 15, no. 10, pp. 3679–3682, 1999.

[111] D. Quéré, "Inertial capillarity," *EPL (Europhysics Letters)*, vol. 39, no. 5, p. 533, 1997.

[112] O. Shardt, P. R. Waghmare, J. Derksen, and S. K. Mitra, "Inertial rise in short capillary tubes," *RSC Advances*, vol. 4, no. 28, pp. 14 781–14 785, 2014.

[113] S. Schiaffino and A. A. Sonin, "Molten droplet deposition and solidification at low weber numbers," *Physics of Fluids*, vol. 9, no. 11, pp. 3172–3187, 1997.

[114] S. Hodges, O. Jensen, and J. Rallison, "Sliding, slipping and rolling: the sedimentation of a viscous drop down a gently inclined plane," *Journal of Fluid Mechanics*, vol. 512, pp. 95–131, 2004.

[115] L. Gao and T. J. McCarthy, "Contact angle hysteresis explained," *Langmuir*, vol. 22, no. 14, pp. 6234–6237, 2006.

[116] P. Aussillous and D. Quéré, "Liquid marbles," *Nature*, vol. 411, no. 6840, pp. 924–927, 2001.

[117] A. J. Griggs, A. Z. Zinchenko, and R. H. Davis, "Creeping motion and pending breakup of drops and bubbles near an inclined wall," *Physics of Fluids*, vol. 21, no. 9, p. 093303, 2009.

[118] P. R. Waghmare and S. K. Mitra, "Needle-free drop deposition technique for contact angle measurements of superhydrophobic surfaces," *Journal of Applied Physics*, vol. 116, no. 11, p. 114903, 2014.

[119] A. S. Utada, E. Lorenceau, D. R. Link, P. D. Kaplan, H. A. Stone, and D. A. Weitz, "Monodisperse double emulsions generated from a microcapillary device," *Science*, vol. 308, no. 5721, pp. 537–541, 2005.

[120] S. H. Kim, J. W. Kim, J. C. Cho, and D. A. Weitz, "Double-emulsion drops with ultra-thin shells for capsule templates," *Lab Chip*, vol. 11, pp. 3162–3166, 2011.

[121] A. J. Griggs, A. Z. Zinchenko, and R. H. Davis, "Gravity-driven motion of a deformable drop or bubble near an inclined plane at low reynolds number," *International Journal of Multiphase Flow*, vol. 34, no. 4, pp. 408–418, 2008.

[122] K. Y. Law and H. Zhao, *Surface wetting: characterization, contact angle, and fundamentals*. Springer, 2015.

[123] Q. Li, P. Zhou, and H. Yan, "Pinning–depinning mechanism of the contact line during evaporation on chemically patterned surfaces: a lattice boltzmann study," *Langmuir*, vol. 32, no. 37, pp. 9389–9396, 2016.

[124] S. Dash and S. V. Garimella, "Droplet evaporation dynamics on a superhydrophobic surface with negligible hysteresis," *Langmuir*, vol. 29, no. 34, pp. 10 785–10 795, 2013.

[125] R. Picknett and R. Bexon, "The evaporation of sessile or pendant drops in still air," *Journal of Colloid and Interface Science*, vol. 61, no. 2, pp. 336–350, 1977.

[126] D. Orejon, K. Sefiane, and M. E. Shanahan, "Stick–slip of evaporating droplets: substrate hydrophobicity and nanoparticle concentration," *Langmuir*, vol. 27, no. 21, pp. 12 834–12 843, 2011.

[127] X. Chen, R. Ma, J. Li, C. Hao, W. Guo, B. L. Luk, S. C. Li, S. Yao, and Z. Wang, "Evaporation of droplets on superhydrophobic surfaces: Surface

roughness and small droplet size effects," *Physical Review Letters*, vol. 109, no. 11, p. 116101, 2012.

[128] Y.-C. Chuang, C.-K. Chu, S.-Y. Lin, and L.-J. Chen, "Evaporation of water droplets on soft patterned surfaces," *Soft matter*, vol. 10, no. 19, pp. 3394–3403, 2014.

[129] H. P. Jansen, H. J. Zandvliet, and E. S. Kooij, "Evaporation of elongated droplets on chemically stripe-patterned surfaces," *International Journal of Heat and Mass Transfer*, vol. 82, pp. 537–544, 2015.

[130] C. Bourges-Monnier and M. Shanahan, "Influence of evaporation on contact angle," *Langmuir*, vol. 11, no. 7, pp. 2820–2829, 1995.

[131] J. Maxwell, *The collected scientific papers of James Clerk Maxwell*. Dover, 1890.

[132] K. Birdi, D. Vu, and A. Winter, "A study of the evaporation rates of small water drops placed on a solid surface," *Journal of Physical Chemistry*, vol. 93, no. 9, pp. 3702–3703, 1989.

[133] Y. O. Popov, "Evaporative deposition patterns: spatial dimensions of the deposit," *Physical Review E*, vol. 71, no. 3, p. 036313, 2005.

[134] G. McHale, S. Aqil, N. Shirtcliffe, M. Newton, and H. Y. Erbil, "Analysis of droplet evaporation on a superhydrophobic surface," *Langmuir*, vol. 21, no. 24, pp. 11 053–11 060, 2005.

[135] S. Dash, N. Kumari, and S. Garimella, "Characterization of ultrahydrophobic hierarchical surfaces fabricated using a single-step fabrication methodol-

ogy," *Journal of Micromechanics and Microengineering*, vol. 21, no. 10, p. 105012, 2011.

[136] M. E. Shanahan, "Simple theory of" stick-slip" wetting hysteresis," *Langmuir*, vol. 11, no. 3, pp. 1041–1043, 1995.

[137] A. N., P. M., and N. S., "Evaporating drops on patterned surfaces: Transition from pinned to moving triple line," *J. Colloid Interface Sci.*, vol. 337, no. 1, pp. 176–182, 2009.

[138] E. Dietrich, E. S. Kooij, X. Zhang, H. J. Zandvliet, and D. Lohse, "Stick-jump mode in surface droplet dissolution," *Langmuir*, vol. 31, no. 16, pp. 4696–4703, 2015.

[139] P. Weisensee, N. Neelakantan, K. Suslick, A. Jacobi, and W. King, "Impact of air and water vapor environments on the hydrophobicity of surfaces," *J. Colloid Interface Sci.*, vol. 453, pp. 177–185, 2015.